A Novel Mouse Model for the study of Spinal Cord Injury-associated Heterotopic Ossification

Rachad Aita, Experimental Surgery

Department of Surgery

McGill University, Montreal, QC, Canada

April 2023

A thesis submitted to McGill University in partial fulfillment of the requirements for the degree of Master of Science in Experimental Surgery

TABLE OF CONTENTS:

ABSTRACT:

Background:

About 900,000 individuals suffer a traumatic spinal cord injury (SCI) every year. SCI severely impacts the quality of life and increases the risk for debilitating sequelae. One increasingly recognized complication of SCI is heterotopic ossification (HO): the abnormal and painful formation of bone in soft tissues. Currently the only curative treatment for HO, surgical excision may become complicated by abnormal bone entrapping nerves and blood vessels, furthering the burden of the disease. Due to the knowledge gap in HO pathophysiology, current pharmacological strategies are non-specific and suboptimal in relieving chronic pain or preventing recurrence after initial resection. To study the pathophysiology of HO, several animal models have been developed. The only existing mouse model for SCI-associated HO utilizes injection of cardiotoxin, a protein extracted from snake venom, to induce periarticular injury. However, cardiotoxin primarily affects muscle cells and not the surrounding tissue; hence this model does not recapitulate the polytraumatic injuries which typically precede HO formation. The lack of a clinically relevant preclinical animal model creates a barrier for the mechanistic studies of SCI-associated HO to develop novel therapeutics.

Goal:

This project aims to develop a novel murine model of SCI-associated HO using concurrent traumatic muscle and tendon injury (MTI).

Methods:

Ten-week-old C57BL/6J female mice were subjected to a spinal cord transection at T9-T10 to induce an SCI, followed by a musculotendinous injury (MTI) by crushing and transecting the left

quadriceps muscle and tendon (n=17). All right hindlimbs were uninjured and served as internal procedural controls. Mice were euthanized after 1 (n=7) and 4 weeks (n=10), and high-resolution micro-CT scans of hindlimbs were performed to quantify HO volumes and native femur bone quality. Collected samples were then embedded in methyl methacrylate, and consecutive 5μm sections were obtained and stained with Von Kossa for mineralized soft tissues, alkaline phosphatase (ALP) for osteoblast activity, and tartrate-resistant acid phosphatase (TRAP) for osteoclast activity.

Results:

Quantitative micro-CT analysis at 1 and 4 weeks showed that SCI+MTI led to significantly higher ectopic mineral volumes (in 10^7 μm^3) than SCI alone at 1 week (median, Q1 – Q3: 5.67, 2.58 – 8.38 vs. 0.324, 0.265 – 0.345, $p=0.0111$), and at 4 weeks (median, Q1 – Q3: 8.72, 6.96 – 17.0 vs. 0.26, 0.186 – 0.270, $p<0.0001$). Mice with SCI displayed significant thinning of femoral cortical bone and reduced trabecular bone volumes in comparison to non-SCI mice. At loci of ectopic mineral formation in SCI+MTI mice, only TRAP activity colocalized with mineral deposits at 1 week. ALP and TRAP staining showed colocalization of osteoblast and osteoclast activity at the site of ectopic bone formation at 4 weeks. A sharp increase in ALP activity, but not TRAP activity, is noted from 1 to 4 weeks only following SCI+MTI.

Conclusion:

These findings suggest that we have successfully developed and established a novel mouse model for abnormal bone and mineral formation following SCI. This study represents a novel preclinical model of SCI-induced HO and mineral formation to study pathogenic mechanisms and assess novel therapies.

RÉSUMÉ :

Introduction :

Chaque année, environ 900 000 personnes subissent une lésion traumatique de la moelle épinière (LME). La LME affecte gravement la qualité de vie et augmente le risque de séquelles débilitantes. Une complication de plus en plus reconnue des LME est l'ossification hétérotopique (OH) : la formation anormale et douloureuse d'os dans les tissus mous. L'excision chirurgicale peut se compliquer du fait que l'os anormal emprisonne des nerfs et des vaisseaux sanguins, ce qui alourdit encore le fardeau de la maladie. En raison du manque de connaissances sur la physiopathologie de l'OH, les stratégies pharmacologiques actuelles sont non spécifiques et sous-optimales pour soulager la douleur chronique ou prévenir la récurrence après l'excision. Plusieurs modèles animaux ont été développés pour étudier la physiopathologie de l'OH. Le seul modèle de souris existant pour l'OH associée à une LME utilise l'injection de cardiotoxine, une protéine extraite du venin de serpent, pour induire une lésion périarticulaire. Cependant, la cardiotoxine affecte principalement les cellules musculaires et non les tissus environnants ; ce modèle ne récapitule donc pas les lésions polytraumatiques qui précèdent généralement la formation de l'OH. L'absence d'un modèle animal préclinique pertinent sur le plan clinique constitue un obstacle aux études mécanistiques de l'OH associée à une LME en vue de mettre au point de nouvelles thérapies.

Objectif :

Ce projet vise à développer un nouveau modèle murin d'OH associée à une LME en utilisant des lésions traumatiques simultanées des muscles et des tendons (LMT).

Méthodes :

Des souris femelles C57BL/6J âgées de dix semaines ont été soumises à une transection de la moelle épinière à T9-T10 pour induire une LME, suivie d'une lésion musculo-tendineuse (LMT) par écrasement et transection du muscle et du tendon du quadriceps gauche (n=17). Tous les membres postérieurs droits n'ont pas été blessés et ont servi de contrôles de procédure internes. Les souris ont été euthanasiées après 1 (n=7) et 4 semaines (n=10), et des analyses micro-TDM à haute résolution des membres postérieurs ont été réalisés pour quantifier les volumes d'OH et la qualité de l'os fémoral natif. Les échantillons prélevés ont ensuite été enrobés dans du méthacrylate de méthyle, et des sections consécutives de 5µm ont été obtenues et colorées avec la Von Kossa pour les tissus mous minéralisés, la phosphatase alcaline (ALP) pour l'activité des ostéoblastes, et la phosphatase acide résistante au tartrate (TRAP) pour l'activité des ostéoclastes.

Résultats :

L'analyse quantitative par micro-TDM à 1 et 4 semaines a montré que LME+LMT entraînait des volumes de minéraux ectopiques (en 10^7 μm^3) significativement plus élevés que LME seule à 1 semaine (médiane ; Q1 – Q3 : 5.67, 2.58 – 8.38 vs 0.324, 0.265 – 0.345, p=0.0111), et à 4 semaines (médiane ; Q1 – Q3 : 8.72, 6.96 – 17.0 vs. 0.26, 0.186 – 0.270, p<0.0001). Les souris atteintes de lésions médullaires présentaient un amincissement significatif de l'os cortical fémoral et une réduction du volume de l'os trabéculaire par rapport aux souris non atteintes de lésions médullaires. Aux endroits de formation minérale ectopique chez les souris LME+LMT, seule l'activité TRAP était colocalisée avec les dépôts minéraux à une semaine. Les colorations ALP et TRAP ont montré une colocalisation de l'activité des ostéoblastes et des ostéoclastes sur le site de formation osseuse ectopique à 4 semaines. Une forte augmentation de l'activité ALP, mais pas de l'activité TRAP, est notée entre 1 et 4 semaines seulement après LME+LMT.

Conclusion :

Ces résultats suggèrent que nous avons développé et établi avec succès un nouveau modèle de souris pour la formation anormale d'os et de minéraux à la suite d'une lésion médullaire. Cette étude représente un nouveau modèle préclinique de formation osseuse et minérale induite par une lésion médullaire pour étudier les mécanismes pathogènes et évaluer de nouvelles thérapies.

ACKNOWLEDGMENTS

My deepest gratitude goes to my supervisors Dr. Chan Gao, Dr. Rahul Gawri, and Dr. Edward Harvey, whose mentorship and continuous guidance have helped me nurture the scientific thinking and critical approach to express my fondness for translational science. Without their help, the culmination of this scientific work would not have been possible.

I am also grateful for the direction and counsel of committee members Dr. Lisbet Haglund and Dr. Derek Hadar Rosenzweig, for providing critical directional input for the project.

A big note of thanks to all the students on the C10 Floor at the Montreal General Hospital for maintaining a fruitful and positive work environment. I'd like to specifically acknowledge the exceptional help of Ailian Li, the nicest bone histopathology expert!

Finally, I would like to extend a note of thanks to my family for their support and patience throughout this journey, including my parents, my brothers, and sister, as well as my close friends who pushed me to never settle for less than 100%.

CONTRIBUTION OF AUTHORS:

The following thesis is written in a manuscript-based format complying with the requirements of the thesis guidelines established by McGill University's Graduate and Postdoctoral Studies Office (GPSO). A comprehensive review of the literature for this research is included in Chapter 1. The original experimental work is presented in Chapter 3 and is formatted as a manuscript in preparation for submission. The data presented in Chapter 3 is part of this manuscript-based thesis only and no other thesis contains this data. The technique and research questions were developed by the author with the help of their supervisors. The majority of the experiments, data collecting, and analysis were also performed by the author. The author wrote the manuscript and generated the figures under the direction of their supervisors. Co-author contributions to the manuscript are outlined below.

Rachad Aita performed perioperative planning, perioperative animal care, post-surgical tissue processing, micro-CT scanning, tissue embedding, sectioning, and histological staining. Rachad also performed the statistical analysis and wrote the manuscript.

Tarek Klaylat helped perform the histological staining and quantification and helped format the manuscript for publication.

Joseph A. Petruccelli developed unpublished preliminary results under the supervision of Dr. Gao which helped guide the rationale for the novel animal model in Chapter 3.

Guillaume St-Jean shared his expertise in animal models development and histological data interpretation.

Mohan Radhakrishna shared his expertise in medical complications of spinal cord injury and provided funding support for histological study.

Dr. Rahul Gawri secured funding, provided lab space, crucial materials, and oversaw all experimental procedures performed. Dr. Gawri mentored the author, co-supervised the entire thesis, and helped prepare the manuscript and approved the final version for submission.

Dr. Chan Gao secured funding, provided lab space, crucial materials, taught and performed the surgical procedures, oversaw the entirety of the thesis from conception to reality, and mentored the author throughout the whole process. Dr. Chan Gao edited the manuscript and finalized it for publication.

LIST OF FIGURES AND TABLES

CHAPTER 1:

CHAPTER 2:

CHAPTER 3:

ABBREVIATIONS

2D: Two Dimensional

3D: Three Dimensional

AHO: Albright's Hereditary Osteodystrophy

ALP: Alkaline Phosphatase

BMP: Bone Morphogenetic Protein

BV/TV: Bone Volume over Total Volume

CCAC: Canadian Council on Animal Care

CNS: Central Nervous System

COX-1: Cyclooxygenase-1

Ct. B.Ar: Cortical Bone Area

CT: Computed Tomography

CTX: Cardiotoxin

DC: Dystrophic Calcification

ECM: Extracellular Matrix

EMT: Epithelial-to-Mesenchymal Transition

EO: Endochondral Ossification

ER: Extended Release

FACC: Facility Animal Care Committee

FAP: Fibroadipogenic progenitors

FOP: Fibrodysplasia Ossificans Progressiva

FoxD1: Forkhead box d1

Fx: Fracture

Glast: Glutamate aspartate transporter

Gli1: Glioma-associated oncogene 1

GNAS: Guanine Nucleotide binding protein, Alpha Stimulating activity polypeptide

H&E: Hematoxylin & Eosin

HO: Heterotopic Ossification

Inj: Injection

IO: Intramembranous Ossification

LDR: Low Dose Radiation

MTI: Musculotendinous Injury

Mx1: Myxovirus resistance-1

NHO: Neurogenic HO

NSAIDs: Non-Steroidal Anti-Inflammatory Drugs

OSM: Oncostatin M

Pax1: Paired box 1

PDGFRα: Platelet-Derived Growth Factor Receptor alpha

PFA: Paraformaldehyde

POH: Progressive Osseous Heteroplasia

PPHP: Pseudopseudohypoparathyrodism

Prx1: Paired related homeobox-1

PXE: Pseudoxanthoma elasticum

RCT: Randomized Clinical Trials

ROI: Region of Interest

ROM: Range-Of-Motion

Runx2: Runt-related transcription factor 2

SCI: Spinal Cord Injury

Scx: Scleraxis

SEM: Standard Error of Mean

SOX9: SRY-box 9

T9-T10: Thoracic 9 and thoracic 10

TBI: Traumatic Brain Injury

THA: Total Hip Arthroplasty

Tie2: Angiopoietin-1

TRAP: Tartrate-Resistant Acid Phosphatase

VK: Von Kossa

VOI: Volume of Interest

Wnt1: Wingless and Int-1

Wpi: Week post-injury

CHAPTER 1: INTRODUCTION

1. Heterotopic ossification

1.1. Classification and epidemiology

Heterotopic ossification (HO) is defined as the pathological formation of bone in soft tissues (1). HO is broadly categorized into three types: genetic, traumatic, and neurogenic HO (2). Genetic HO is the rarest of HO types and includes conditions such as Fibrodysplasia Ossificans Progressiva (FOP) prevalent in one in two million births (3), Progressive Osseous Heteroplasia (POH) considered an ultrarare condition (4), and Albright's hereditary osteodystrophy (AHO) (5). AHO includes Pseudopseudohypoparathyrodism (PPHP) and other conditions with limited literature on their prevalence (6). FOP, also called the Stone Man syndrome, is caused by point mutations in the Activin A receptor type I (*ACVR1*) gene, a bone morphogenetic protein (BMP) receptor (7). While both AHO and POH are caused by genetic changes leading to inactivation of the Guanine Nucleotide binding protein, Alpha Stimulating activity polypeptide (*GNAS*) gene, AHO differs in its inheritance pattern (8). Considered a subcategory of traumatic HO, neurogenic HO specifically refers to HO which forms following trauma to the central nervous system (CNS) (9), such as spinal cord injury (SCI), traumatic brain injury (TBI), stroke, and cerebral anoxia.

Among HO types, traumatic HO is the most common form, as patients with non-genetic HO had a history of trauma in up to 75% of HO cases, and the remaining 25% of cases were assumed to involve unreported microtraumas (10). Traumatic HO is most reported in young adults in their early twenties to late thirties, with men being moderately more likely to develop this condition (11). Likewise, neurogenic HO is more commonly reported following SCI and TBI, but less commonly after stroke or other cerebral insults (12). It is of importance to mention that the current literature interchangeably refers to both traumatic and neurogenic HO as acquired HO (13, 14).

Certain factors are recognized to predispose patients to this condition. Orthopedic surgical procedures, like total hip arthroplasty (THA), increase the risk for traumatic HO with HO reported in up to 40% of THA cases (15). Similarly, severe burns and high-energy extremity trauma leading to bone fractures, dislocations, or crush injuries also increase the risk for traumatic HO, with HO reported in ~ 30% of cases (16-18). Moreover, patients with limb amputations represent the highest incidence of traumatic HO formation, with more than 90% of amputations leading to HO as per a United Kingdom-based study (19). Interestingly, the prevalence of neurogenic HO accounts for one of the widest distributions reported for the condition, with HO reported between 10 and 53% of CNS injuries (20, 21). In non-genetic HO, these trends highlighted that the severity of trauma contributed to an increased likelihood of HO formation.

1.2. Clinical manifestation

HO is well documented for its capacity to form at any extra-osseus site; however its traumatic type most commonly presents in soft tissues most prone to injury, such as the periarticular muscles and tendons near the hip, elbow, and knee (22). Moreover, traumatic HO's growth is generally limited to the injured soft tissue, yet HO's bridging to native bone and periosteum, termed periosteal reaction or periosteal HO, is an uncommon occurrence (23).

In the early phase of HO formation, patients may experience pain, tenderness, and swelling due to inflammation (24). As the HO lesion matures, inflammation tends to subside; however, a restricted range of motion of the nearby articulation may occur in severe cases of ossification possibly impairing joint function and entrapping its associated nerves and blood vessels (25).

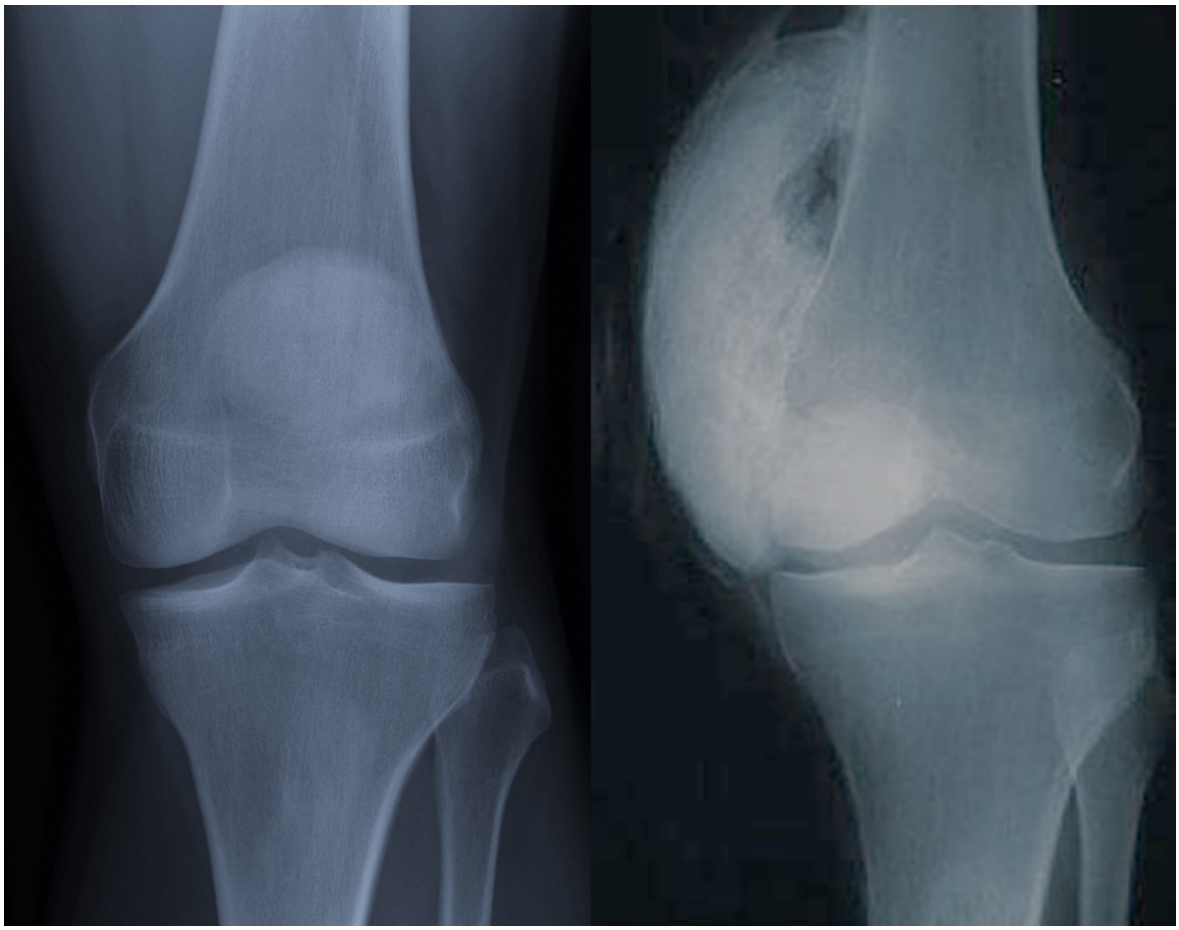

Figure 1. X-ray images of normal knee (left image) and HO-afflicted knee (right image). Left image adapted from www.radiopedia.com (*Case courtesy of Dr. Dixon A, Radiopedia.org, rID 36689*) and right image reproduced with permission from Medscape Drugs & Diseases (https://emedicine.medscape.com/)

In neurogenic HO, the likelihood of developing this condition is highest in patients with low cervical or high thoracic spinal cord lesions. Individuals who have severe spasticity, decubitus ulcers, urinary tract infections, long bone fractures and microtraumas are more susceptible (12). Neurogenic HO incidence can vary between 10 to 50% depending on the neurological injury (26). SCI-induced HO was reported to occur in 20-50 % of cases, while TBI-induced HO was reported

in 10-20% of cases (22). TBI-associated HO incidence may increase to more than 50% if the neurological injury cooccurred with peripheral polytrauma like blast and crush injuries (18). On the other hand, there is limited knowledge pertaining to the effect of coccuring SCI and peripheral polytraumas on SCI-associated HO incidence. However, reports show that larger joints are more likely to develop HO lesions in patients with neurological injuries (27). Furthermore, HO following TBI can develop around any joint, including the hip, knee, elbow, and shoulder. In contrast, HO after spinal cord injury typically develops caudal to the level of the lesion. Small joints are rarely affected by neurogenic HO (28). After a TBI, neurogenic HO often develops within a few months and advances over several years. HO is rarely associated with viscera, yet certain types of genetic HO tend to preferentially affect non-periarticular tissues. HO may present in the skin and subcutis like in POH but may also affect injury-prone soft tissues near joints like in FOP. While minor trauma may be sufficient to induce discrete flares in genetic HO, gradual ossification can occur without any apparent trigger and abnormal bone may fuse with the native skeleton (29).

Genetic HO's propensity for injury-prone soft tissues poses interesting questions. Furthermore, the consistent involvement of periarticular soft tissues and the lack-thereof in other sites of the body in a large proportion of traumatic HO-affected individuals warrants the investigation of tissue-specific capacities for HO initiation and formation.

1.3. Diagnosis

Radiography is a classically used imaging modality for the detection of bone and bone-like radiodensities, because bone does not readily transmit x-rays and appears opaque in relation to the surrounding soft tissue (30). Because early HO lesions are immature, they may initially appear

granular in shape on radiographs. As HO lesions mature, more distinctive and well-define boarders start to emerge in later stages of the disease thereby facilitating diagnosis. Moreover, bridging to native bone becomes more discernable in radiographs (31). Interestingly, the structure of the soft tissue that harbors HO dictates the direction of mineralization and ossification of the abnormal bone (32). HO of the muscle tends to proceed along the axis of myofibers, and HO of the tendon tends to align with the direction of collagen bundles. As for findings which may complicate diagnosis, calcification and ossification are two competing observations on radiographs captured during the condition's intermediate to late phase, as trabeculation and calcification patterns share radiographic commonalities (33).

Although radiographs tend to be the primary imaging modality to visualize HO, computed tomography (CT) scanning is a useful imaging technique for earlier and more accurate diagnosis. CT scanning is a technique which compiles a dataset of high-resolution cross-sections to render 3D reconstructions of an object. These cross-sections, named tomographic images, are generated by X-rays taken at incremental angles relative to the object of interest. CT scanning provides higher resolution imaging of HO lesions than radiographs and thus allows for an earlier and more nuanced characterization of HO morphology and location. CT-scanning may be superior to radiography, as 3D reconstruction and segmentation allows for spatial analysis of the HO lesion to better plan a course of action for disease management (34).

To complement these imaging modalities, histopathological examination of a biopsied lesion provides valuable information at the microscopic level on HO's phase, morphology, and cellular characteristics (35). Using classical staining techniques like hematoxylin and eosin (H&E) to stain nuclei and cytoplasm, early HO lesions predominantly display hypercellularity. Certain cell types and morphologies, such as multinucleated giant cells and inflammatory cells, begin to

surround nodular and mineralized tissue. As HO lesions mature, the zonal architecture of bone may be appreciated, with a stark demarcation from surrounding soft tissues. Staining techniques like Von Kossa (VK), which stains calcium and phosphate in mineral black, provide a useful contrast with surrounding soft tissue to confirm the presence of mineralized and bone-resembling tissue (36). For further confirmation of cellular activity in HO lesions, special histological stains like alkaline phosphatase (ALP) and tartrate-resistant acid phosphatase (TRAP) staining which highlight osteoblast and osteoclast activity, respectively, are often used. ALP and TRAP staining may show the distribution of these bone forming and bone resorbing cells in relation to mineral deposits and permits the analysis of the cellular activity HO lesion (37).

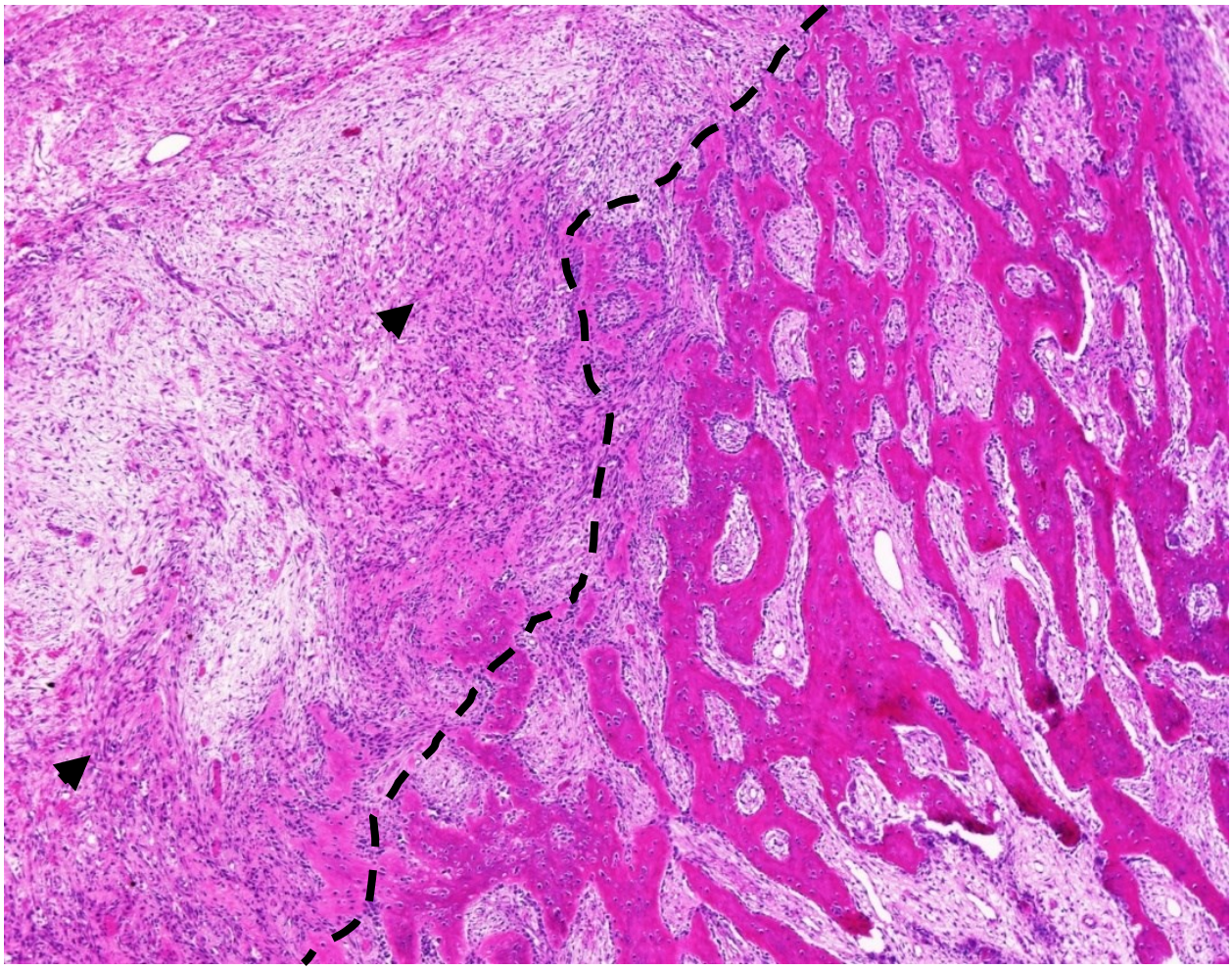

Figure 2. Heterotopic ossification under the microscope after H&E staining.

Black dotted line demarcates the well-defined borders of the HO lesion, Black arrows mark regions of hypercellularity. Image adapted with the permission and courtesy of: WebPathology.com.

Histopathological assessments help distinguish features between HO lesions and bone tumors such as osteosarcomas, as these pathological conditions share some similarities in radiographs features. A defining feature of HO lesions is a well-demarcated compact cortical bone structure as opposed to the poorly defined and cloudy borders of bone tumors. However, more specialized diagnostic modalities are advised to discern between these different conditions (38).

Characterization of these lesions through imaging is an important first step for diagnosis and developing a strategy for disease management.

1.4. Treatment

Due to the unknown etiology of HO, current treatment options are limited. The only curative treatment for HO is surgical resection (24). Yet, insufficient, incomplete, or hasty surgical excision prior to HO maturation may lead to recurrence (39). One study estimated that recurrence after initial excision of HO remains a concern, with 10-15% of resections showing radiographic evidence of HO re-emergence (40, 41). Unfortunately, there are currently no approved non-operative or pharmaceutical interventions which address HO after it has fully developed, but certain management strategies are available for patients with this condition.

Prior to HO maturation, certain preventative measures have previously shown some success, yet opinions differ regarding their efficacy. Drawn from evidence that HO develops more commonly in patients with paralysis, limb motion is theorized to be negatively correlated with HO formation. Patients admitted for post-traumatic recovery are generally prescribed conservative measures, such as physical therapy for range-of-motion (ROM) training, to restore any ambulation

they have left. Some studies showed that ROM training may be somewhat effective in preventing HO; however, other studies suggested that exaggerated or intense bouts of ROM training may aggravate HO (42, 43).

As HO seems closely linked with inflammation, pharmacological prevention methods like the use of non-selective non-steroidal anti-inflammatory drugs (NSAID) were investigated for their efficacy in HO prevention (44). Through the inhibition of cyclooxygenase-1 (COX-1) and COX-2, NSAIDs block the production of prostaglandins, a group of lipid-based molecules which are involved in the generation of an inflammatory response. Case-controlled studies and randomized clinical trials (RCT) involving NSAIDs displayed some success in halting HO progression in its early inflammatory phase (17, 45-48). Resection of early HO lesions is assumed to exacerbate inflammation which can increase the risk of recurrence, thereby reinforcing the importance of inflammation in HO.

Antiresorptive agents, such as bisphosphonates, which inhibit osteoclasts, have been investigated for their effect on HO development. It is hypothesized that targeting osteoclast-dependent calcification in early stages of the disease prevents HO progression. Although bisphosphonates were somewhat successful in preventing HO in some clinical studies, there is no consensus on their efficacy. Current literature seems to advise discretion for their use as they may have off-target affects, possibly impairing pathways affecting native bone homeostasis and fracture healing (49-53).

Low dose radiation (LDR) therapy is a treatment modality which leverages the energy of ionizing radiation to disrupt the DNA of rapidly replicating cells eventually leading to decreased cell proliferation. LDR can be used as a primary intervention to prevent HO in patients at high risk of developing the condition, or as a secondary prevention modality to manage recurrence after

surgical excision. Several studies supported that low dose radiation therapy of 500-700 cGy decreased the incidence of HO following THA. However, there is limited literature exploring the efficacy of LDR for HO prevention near other joints (54-57).

In sum, the current use of non-specific prophylactic measures may result in partial success in preventing HO development. Yet it is unclear whether one prevention modality may be superior to another, and current data suggests a considerable proportion of individuals are unresponsive to these interventions. To address this limitation, investigating the detailed mechanism of HO, and subsequent testing of targeted prophylactic strategies in animal models is essential.

2. Mechanisms of heterotopic ossification

Defining the mechanisms of HO is crucial to understanding different HO initiating processes, pathways underlying disease progression, and the myriad of cellular and molecular interactions that lead to the final disease state. Prior to defining the potential ossification mechanisms of HO, it is important to mention the distinction between abnormal calcification/mineralization and abnormal bone formation.

2.1. Abnormal mineralization

In physiological conditions, mineral concentrations of calcium and phosphate slightly exceed their maximum solubility in most soft tissues, yet mineralization of these tissues does not readily occur. On the other hand, hard tissues (bones) have an inherent physiological capacity to leverage these mineral concentrations to regulate bone mineral density. This dichotomy suggests that the human body contains tissue-specific processes tightly regulated for preventing or inducing mineralization in a timely manner. Therefore, abnormalities in these tissue-specific regulated pathways may stimulate abnormal biomineralization without a systemic mineral imbalance, termed as dystrophic calcification (58).

Several genetic, metabolic, and age-related disorders have been well documented for causing ectopic mineralization unrelated to blunt force trauma (58). These disorders can affect different tissue types such as nephrotic tissue, blood vessels, and other connective tissues (59, 60). One pertinent example is a rare connective tissue disorder called Pseudoxanthoma elasticum (PXE) resulting in mineralization of elastic fibers of the eyes and skin. Simply put, PXE is thought to be linked to mutations in the ATP-binding cassette sub-family C member 6 (*ABCC6*) gene for an efflux transporter leading to a hypothesized downstream deficiency of mineralization inhibitors,

thereby causing an imbalance in activators versus inhibitors of mineralization. This imbalance is considered to favor soft tissue mineralization in PXE (61, 62). Clinical studies measuring serum levels of hypothesized mineralization inhibitors reported lower concentrations of these factors in patients with PXE (62). Furthermore, mouse models which completely knock-out genes for these mineralization-inhibiting proteins showed spontaneous mineralization of arteries and cartilage (63). Although more extensive research is required to understand the detailed pathophysiology of this condition, PXE is a pertinent example to show the possible genetic predispositions which may affect biomineralization.

A second pertinent example of abnormal mineralization pertains to a comorbidity of breast cancer. Imaging modalities like mammography are useful tools to safely screen and diagnose abnormalities in breast tissue. One rare complication which mammography may reveal is microcalcification, estimated to occur in ~1% of patients with breast cancer (64). Microcalcifications are defined as calcium salt deposits in breast cancer tissue and several studies propose mechanisms for the pathological accumulation of these deposits in or near breast cancer lesions. One theory suggests that matrix vesicles, small enclosures of lipid bilayers which pinch off the surface of cells, contain factors that regulate the accumulation of calcium salts (65). Breast cancer cells were shown to have a higher propensity to produce these vesicles and release them in their periphery thereby inducing mineral accumulation and crystallization (66). A second proposed mechanism for microcalcifications in this context explores the capacity of epithelial cells to transdifferentiate into mesenchymal cells with osteoblastic properties. Epithelial-to-mesenchymal transition (EMT) in a subpopulation of breast cancer cells was documented to increase the invasive potential and metastatic quality of breast cancer (67). However, it was unknown whether EMT contributed to microcalcifications in this setting. Furthermore, this subpopulation of mesenchymal

cells in breast cancer tissue displays certain osteoblast-like characteristics, such as the expression of Runt-related transcription factor 2 (Runx2), and production of osteoblast-specific proteins such as osteopontin, and ALP as described in several studies (68-72). These findings propose that a proportion of breast cancer cells may turn into osteoblast-like cells which have a capacity to release mineralization-inducing factors in their matrix (73). Considering these are only proposed pathogenic mechanisms, further studies are required in this setting to confirm the involvement of EMT and osteoblasts in breast cancer microcalcifications.

Abnormal mineralization is a pathological process which seems to occur in many settings of disease but does not necessarily lead to ossification or bone formation. These fields are promising avenues of research to elucidate the tightly regulated pathways for mineral clearance or accumulation which appear organism-wide and, if faulty, may lead to disease.

2.2. Ossification process

Current studies suggest that HO may form in soft tissues by aberrantly activating and hijacking inherent embryological ossification programs (74). In all types of ossification mechanisms, HO is classically theorized to require three factors: an initiating stimulus, an osteopermissive environment, and stem cells with osteogenic capacity (75).

Simply put, HO is currently conceptualized as abnormal soft tissue healing that creates a permissive environment for stem cells to differentiate down the osteogenic lineage. Across HO mechanisms, its pathological process is thought to start with abnormal soft tissue healing that activates faulty debris clearance and abnormal regeneration (76). Differentiated bone forming cells, osteoblasts, then start to deposit unmineralized “prebone” (osteoid) into the extracellular matrix (ECM) (77). Following the gradual mineralization of this osteoid, maturation of the lesion

begins, with some resemblance to native bone. Depending on HO's location, it is documented to form via specific pathways of ossification. This pathological ossification process can be categorized based on its similarities with two main types of ossification extensively studied from embryogenesis: intramembranous and endochondral ossification (78).

a) Intramembranous ossification

Intramembranous ossification (IO) is a classically studied mechanism of ossification in flat bones like those of the skull and the shoulder blades. In IO, BMPs-2, -4 and -7 are important signalling molecules which activate Runx2, a member of the larger family of runt-related factors involved in osteogenesis, to orchestrate the differentiation of stem cells down the osteoblastic lineage (78-80). In intramembranous HO, osteoid is deposited directly into mesenchymal tissue composed of vascularized fibrous membranes of collagen and proteoglycan matrix. Once osteoid has formed in differentiated mesenchymal tissue, binding sites for calcium salts are formed and allow mineral to accumulate. As a result, osteoblasts calcify osteoid and can entrap themselves in this novel calcified matrix resulting in osteocytes residing in their lacunae like that of native bone.

Generally, HO of the dermis is commonly reported to proceed via the intramembranous pathway, as IO is commonly observed in patients with FOP (81). In contrast, periarticular HO may involve a mix of ossification mechanisms. While IO is predominant in intramuscular HO (82), intratendinous HO tends to proceed via endochondral ossification (83-85).

b) Endochondral ossification

The main distinction between intramembranous and endochondral ossification (EO) is the presence of a cartilage intermediate between mesenchymal tissue and unmineralized osteoid,

showcasing the extensively characterized zonal architecture of chondrocytes (cartilage cells) in this ossification mechanism (86). As in IO, BMPs are important signaling molecules involved at all stages of EO's process and exert their effect intracellularly through Smad-dependent signaling transduction (87). In classical EO, mesenchymal cells aggregate and commit to the chondrogenic fate via the concerted action of paracrine factors which activate transcription factors such as paired box 1 (Pax1) and scleraxis (Scx) (88, 89). As cartilage condensations form, upstream Smad-dependent signaling transduction leads to the expression of the SRY-box 9 (SOX9) transcription factor, mediates the chondrogenic cell fate, and directs the next proliferative stage (90). Hyperproliferative chondrocytes begin to secrete a matrix model for bone, followed by the slowing of chondral division and the formation of hypertrophic chondrocytes. Hypertrophic chondrocytes then deposit collagen X and other proteins which permit osteoblast-driven deposition of calcium salts (91). Mineralization and maturation of this tissue then forms the structural foundation of bone which houses bone marrow-resident cells and other cell types (92).

It is important to mention that IO and EO are assumed to occur in HO as they do in embryogenesis due to observed histological similarities. Further studies on HO ossification pathways are required to substantiate these claims and the contribution of stem cells in these proposed mechanisms.

2.3. Osteoprogenitors

Osteoprogenitor cells are stem cells acting as precursors to the osteoblasts and osteocytes that form and maintain bone. Several lineage tracing studies using cre-lox systems, to activate certain cell types in a tissue-specific manner, attempt to elucidate the progenitor cells and requisite stem cell niches which drive HO in different animal models (93). To narrow down the search of

target stem cell populations, other studies focused on deactivating certain cell types thought to be indirectly related to HO initiation (94). Depending on the affected tissue and the type of HO present, an array of stem cell types may be involved to varying degrees and at different stages of HO.

Although there is no consensus on which putative cell types are involved, compounded data so far suggested that scleraxis-1 (Scx1), myxovirus resistance-1 (Mx1), paired related homeobox-1 (Prx1), glutamate aspartate transporter (Glast), angiopoietin-1 (Tie2), glioma-associated oncogene (Gli1), and Wingless and Int-1 (Wnt1) expressing osteoprogenitors among others have been directly linked to different HO types in different mouse models. Some studies revealed that both resident Scx1-expressing stem cells originating from tendon, and Mx1-expressing stem cells originating from muscle interstitium were reported to contribute to HO of the tendon and muscle (95). In another study, Glast-expressing osteoprogenitors originating from connective tissue near blood vessels were reported to be involved at all stages of the zonation pattern in endochondral HO of the subcutis induced by BMP4 and injury. This mouse model also showed that forkhead box d1 (FoxD1)-expressing stem cells of the mesenchymal lineage contributed to the development of normal skeletal bone but not pathological bone (96). This finding may challenge the view that pathological bone formation and normal skeletogenesis are due to the activation of the same ossification pathways; yet further studies are required to investigate these differences. In another study of BMP4-induced intramuscular HO, the endothelium-related Glast and Tie-2, and interstitium-related Gli1-expressing osteoprogenitor cells were reported as the predominant contributors of HO's stem cell niche, with Glast and Gli1-expressing stem cells being the predominant osteoprogenitors. Depleting Glast-expressing stem cells in this mouse model decreased HO incidence from 100% to 60%, thereby highlighting the

importance of these stem cells for HO but also suggesting that other stem cell types are involved (97). In another study, Wnt1-expressing stem cells originating from the endoneurium, the interior layer of connective tissue in the nerve sheath that contains peripheral nerve fibers, were reported to contribute to endochondral HO induced by BMP2. This study then examined a subset of the Wnt-1-expressing stem cells who co-express osterix, a transcription factor known to drive differentiation of mesenchymal stem cells down the osteoblastic lineage (98). Although these nerve-originating stem cells were reported be involved in BMP2-induced HO, the role of these stem cells in HO following central neurological injury is yet to be investigated. Additionally, other studies proposed that circulating and not resident mesenchymal stem cells of non-hematopoietic origin also played a role in HO formation (99-102). Given the state of current literature on HO osteoprogenitors, it seems unlikely that a single putative cell type solely contributes to HO formation, which emphasizes the complexity of this condition.

Recent advances in a mouse model of SCI-associated HO reported the importance of a subset of progenitors with fibroblastic and adipogenic potential, termed fibroadipogenic progenitors (FAP) in HO. These labelled FAPs co-expressed Prx1 and platelet-derived growth factor receptor alpha (PDGFRα) and were shown to drive ectopic bone formation in a cardiotoxin-induced SCI-associated HO model. Interestingly, these progenitors were reported to be abnormally maintained by environmental factors yet to be explored (103).

2.4. Microenvironment

The microenvironment of HO is generally defined as the microscopic environment containing important mediating factors, supportive cell types, and physiological structures permitting HO's disease process. Defined as microenvironments which permit osteogenic activity,

osteopermissive environments have been subject of intense study for their contribution to "niche factors" and their myriad cellular and molecular interactions on HO initiation and progression.

Following tissue damage and hypoxia, inflammation is considered an essential factor for HO development. This is emphasized by the success of preventative strategies such as NSAIDs and selective COX inhibitors which target early inflammatory stages of HO. Drawing from this premise, the innate immune system is a likely contributor to inflammation in HO's early stages; specifically, the role of macrophages in HO has recently been under investigation. By using the macrophage apoptosis inducer, clodronate, depletion of macrophages was able to partially inhibit HO formation in models of SCI-associated HO, HO by BMP4 overexpression, and by ACVR1 knock-in (100, 104, 105). To investigate which secreted factors from macrophages are involved in HO development, one study highlighted the expression, close association, and involvement of Oncostatin M (OSM), an osteoblast-inducing cytokine, derived from macrophages in HO formation both *in vivo* and *in vitro* (106). Continuing the search for innate immunity's role in HO, other studies were interested in the role of granulocytes in HO formation. Some studies have shown that mast cells contribute significantly to HO formation, as was shown in a mouse model of HO by BMP2 administration. Inhibiting the degranulation of mast cells by Cromolyn was able to reduce HO formation in this mouse model (107, 108). Cells of the innate immune system seem to be important supportive cell types for HO; however, it was unclear whether adaptive immunity also played a role. One study using cardiotoxin-induced SCI-associated HO investigated the involvement of lymphocytes. Mature T and B lymphocyte depletion by splenectomy showed no significant effect on HO development, as depletion of these cells did not affect HO bone volumes (109). While this highlights that the presence of maturing lymphocytes is not required in SCI-associated HO, other studies which impair early development of T and B lymphocytes by

Recombination activating gene 1 (Rag1) deficiency showed reduced HO formation induced by burn and tenotomy (110).

These studies implicitly show that the method of injury and subsequent HO type may influence findings on the immune system's contribution to HO. It is yet to be detailed how adaptive immunity comes into play in different HO types by different methods of induction.

Besides immunity, studies showed that other cells are considered requisite cell types to form an osteopermissive microenvironment; these are termed stem cell niches. Stem cell niches are composed of stem cells as mentioned above, and other differentiated cell types which maintain a nutritious and permissive microenvironment for different stages of the disease. In a study of BMP4 and cardiotoxin-induced HO, the spatial relationship of vascular endothelial cells, neuronal fibers, mast cells and macrophages with HO's stem cell niche was investigated. Although only macrophages were observed to colocalize with labelled stem cells as early as the condensation stage of HO, vasculature, neurites, and mast cells were additionally observed in close association (97). This not only reinforces the early role of macrophages and proposes their contribution to this stem cell niche, but also sheds light on the importance of blood vessels and nerves. As such, certain cell types are required to varying degrees depending on HO's stage, and further studies are required to elucidate their cellular and molecular contributions to HO's process.

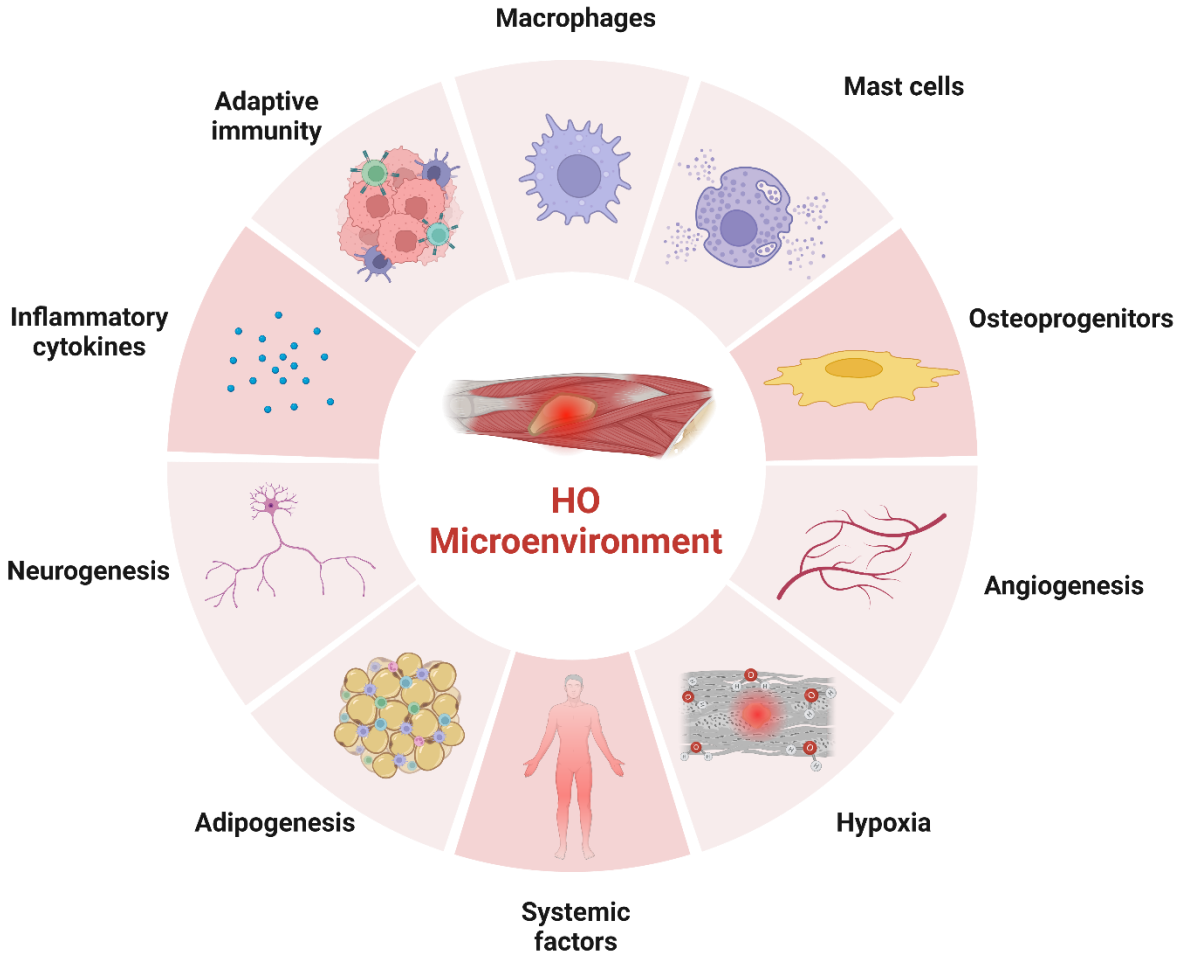

Figure 3. Microenvironment of heterotopic ossification.

(Created with BioRender.com)

From these HO stem cell niche studies, it has become readily apparent that findings may vary depending on the type of HO induced. Due to the plethora of methods available for disease emulation, it is paramount for therapy testing that mouse models accurately recapitulate the clinical scenario of the intended type of HO.

3. Animal Models of Heterotopic Ossification

3.1. Types of models

Animal models are critical tools for investigating the disease mechanism and evaluating prospective treatments for HO. They are a necessary substitute for human HO studies because early resection increases the risk of HO recurrence.

Models of HO are categorized by the type of HO they mimic, and include models of genetic, BMP-inducible, traumatic, and neurogenic HO (111). Noted for the practicality of their application, models of genetic HO utilize mice with mutations at ortholog loci known to contribute to aberrant bone formation in humans. Among the most popular HO models, inducible models inject BMPs into soft tissue to cause localized HO. Mimicking the most common type of HO in humans, traumatic HO models use traumatic injuries as the aberrant trigger for initiating ossification of damaged soft tissue. Neurogenic HO models, a subclass of traumatic HO models, use concurrent traumatic injuries to the CNS and peripheral soft tissues. Although induction techniques for several HO categories may overlap, HO is most frequently initiated after a combination of induction modalities.

Currently, studies simulating a FOP-like phenotype commonly use two models of genetic HO. These models either utilize mice with mutated Acvr1 R206H (arginine at amino acid position 206 replaced by histidine) or Acvr1 Q207D (glutamine at amino acid position 207 replaced by aspartic acid), and both mutations lead to hyperactivity of BMP signaling (112-116). Although this knock-in mutations leads to body-wide expression of the defective allele, it may be combined with a traumatic injury to accelerate site-specific ossification. In contrast, the use of cre-inducible tissue-specific mouse models provide a more accurate and controlled FOP phenotype (115). This

novel generation of transgenic mouse models provides a new platform to test novel therapies and study the contribution of putative cell types to HO formation.

As with genetic HO models, BMP-induced models leverage the hyperactivity of BMP signaling (117-120). BMP-induced models exhibit similar adaptability in their application, with BMP2 or 4 most employed (120). Furthermore, the targeted and localized injection of BMPs, BMP-loaded vehicles, or stem cells constitutively expressing BMPs allows for the mitigation of off-target effects. Moreover, BMPs can be delivered to any site to study a specific tissue's propensity for HO formation. However, because of the potential for soft tissue injury from injection, BMP-induced models of HO have limitations. Nonetheless, they are frequently employed to examine HO's disease process following BMP hyperactivity and test suggested therapeutic approaches.

Granted by their ability to circumvent the use of foreign substances to cause HO, traumatic HO models may represent clinically relevant models for the condition's traumatic form. Similar to the increased proclivity of polytrauma patients to develop HO, blunt force trauma resulting in severe injuries seems sufficient to simulate HO in genetically unmodified mice, while mild injuries seldom cause aberrant ossification (121-123). These combined injuries may include soft tissue burns and crush injuries, thereby accurately mimicking HO's most common predisposing conditions. A commonly used mouse model for traumatic HO employs combined burn injuries to the dorsal trunk and transection of the Achilles tendon (122). Furthermore, recent studies on HO's pathogenic mechanism combined BMP injections and soft tissue injuries to exacerbate HO formation (124). Although it is evident that there could be a multitude of methods for inducing traumatic HO, few animal models exist to accurately study neurogenic HO: HO following central neurological injury.

	Neurogenic HO			Traumatic HO			BMP-induced HO			FOP	POH
Method of induction	TBI + Fx + Muscle Crush	SCI + Muscle + Tendon Crush	SCI + CTX	Burn + Tenotomy	Blast + Fracture + Amputation	THA	BMP2 inj. + SCI	BMP2 Implant	BMP4 Inj.	Acvr1 knock-in	GNAS knock-in
Animal Host	Rat	Mouse	Mouse	Mouse	Rat	Rabbit	Mouse	Mouse	Mouse	Mouse	Chicken

Table 1 – Animal models of heterotopic ossification.

3.2. Models of neurogenic heterotopic ossification

As their unique and defining feature, traumatic and neurogenic HO (NHO) models are the only models which rely mainly on trauma to induce HO. There are two primary categories of neurogenic HO models: those that resemble HO after TBI and those that imitate HO after SCI.

Animal models of HO following CNS injury have been developed, and these models combine CNS trauma with periarticular injury. It is interesting to note that the process of ossification in peripheral tissues following HO from CNS damage has not yet been identified; as a result, it is currently uncertain whether endochondral, intramembranous, or dystrophic calcification-rich lesions predominate. In an effort to develop a model that could enable the study of HO following TBI, NHO has been examined in rats with concomitant TBI and peripheral injuries (125). These peripheral injuries mimicked femoral fractures and muscle injuries frequently seen in TBI patients. At 6 weeks post-injury, 70% of rats who underwent combined injuries with TBI were found to have ectopic bone in the wounded hindlimb. However, 20% of the rats who received peripheral injuries without TBI also developed ectopic bone within the same period. While this mouse model aims to emulate TBI-associated HO, it could be argued that it preferentially induces non-neurogenic HO in a smaller proportion of injured rats (125). For this

mouse model to mimic neurogenic HO, single peripheral injuries ought not to form HO, but should only do so in the context of combined TBI and peripheral injuries.

To mimic neurogenic HO, one study employs mice with concomitant SCI and BMP2 injections (126). However, previous studies showed that the use of BMP2 alone was sufficient to induce HO (120), which puts into question the relevance of using an SCI in a BMP-induced HO context. Since this model resembles BMP-induced models more than the neurogenic type, it is useful to investigate the concurrent effect of a SCI on BMP-induced HO.

Currently, only the mouse model established by Genet and Levesque for neurogenic HO is phenotypically distinct from other HO models (105). This model is useful in demonstrating the required concomitance of SCI and muscle inflammation for aberrant ossification to take place. Furthermore, this mouse model was involved in numerous studies to examine the unique pathogenic mechanism of neurogenic HO. This model helped elucidate a third mechanism of ossification in HO, one that may be specific to neurogenic HO: the gradual ossification of dystrophic calcification-rich lesions. Although examining the contribution of muscle inflammation to HO deepens our understanding of this condition, the use of cardiotoxin introduces an exogenous chemical that may interfere with HO's pathogenic mechanism in mice. Snake venom-derived cardiotoxin primarily affects contractile bundles of muscle and less so other surrounding soft tissues like nerves, blood vessels, and fat (127). Furthermore, it is unlikely that patients with neurogenic HO suffer from isolated peripheral muscle injuries; they most likely suffer from simultaneous injuries to other soft tissues as well (128-130). As such, the contribution of other tissue types in the context of polytrauma may be inadvertently excluded in this model, which may hinder our understanding of neurogenic HO and its microenvironment.

Therefore, the development of an animal model which employs polytraumatic periarticular injuries in the context SCI is critical to study the detailed pathophysiology of NHO as seen in human patients.

CHAPTER 2: RATIONALE, HYPOTHESIS, AND GOAL

1. Rationale

Current clinical research on SCI-associated HO is mainly retrospective which provides limited insight into the pathogenesis. Surgical resection is only indicated for mature HO to avoid postoperative recurrence (131). Due to this necessary delay, the study of these resected lesions may only reveal the latent mediators of this condition rather than its initiating factors, making early pathophysiological and prospective studies in humans unfeasible. Hence, the pathogenic mechanisms of SCI-associated HO are yet to be understood.

Animal models have been critical in gaining a preliminary understanding of the early and latent mediators of HO lesions. Moreover, current models are especially valuable in simulating the combined CNS and periarticular injuries needed to induce neurogenic HO. However, the clinical scenario of polytrauma is not accurately reflected with the current methods of periarticular injury in animal models. In humans, risk factors for developing SCI-associated HO include spasticity, pressure sores, and mechanical stress at periarticular sites. Yet, previous models for SCI-associated HO administer exogenous substances like cardiotoxin to elicit muscle inflammation. Therefore, the development of a novel animal model that employs only mechanical injury at periarticular sites is essential to facilitate the accurate study of SCI-associated HO and test novel therapies for this condition.

2. Hypothesis

We hypothesized that concomitant traumatic musculotendinous injury (MTI) and SCI leads to SCI-associated HO.

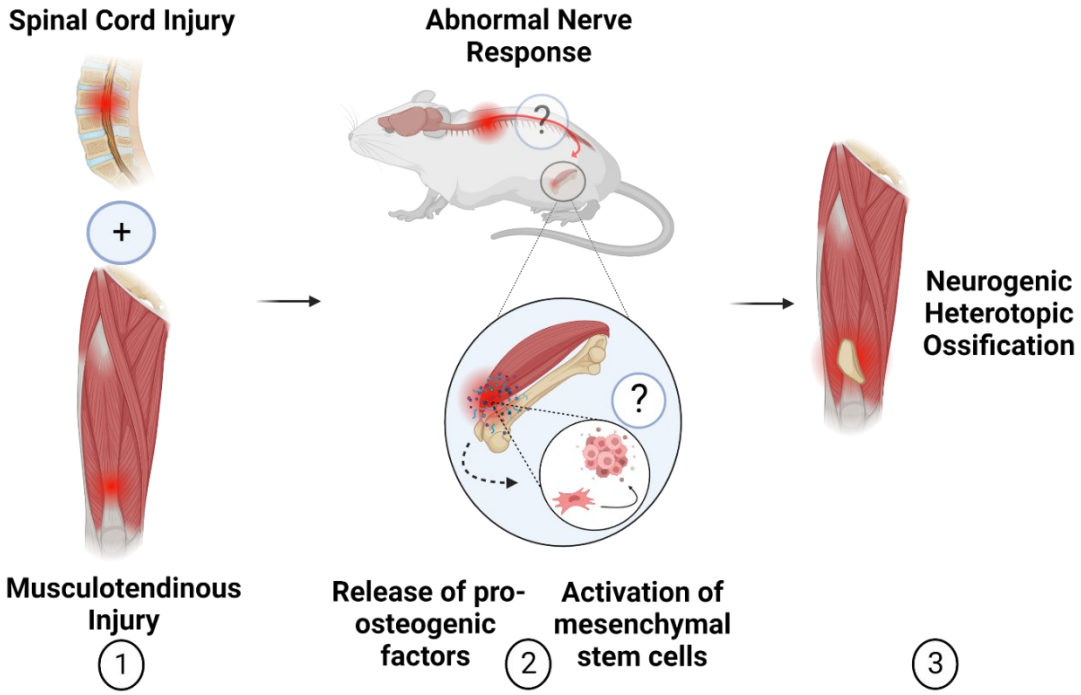

Figure 1. Proposed mechanism for SCI-associated HO.

(Created with BioRender.com)

3. Goal

This study aimed to develop a reproducible surgical protocol to perform concomitant MTI and SCI, and to characterize the SCI-associated HO in this novel mouse model.

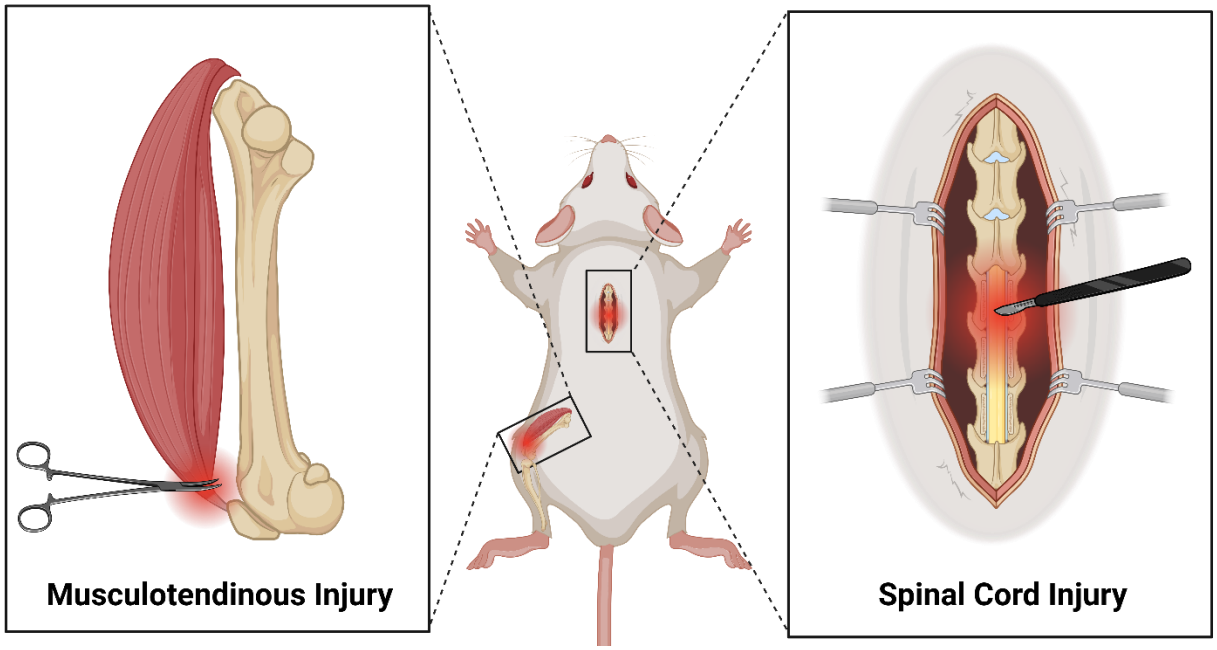

Figure 2. Surgical design in our mouse model of SCI-associated HO.

(Created with BioRender.com)

CHAPTER 3: Spinal Cord Injury-associated Heterotopic Ossification – A Novel Mouse Model

Authors and Affiliations:

Rachad Aita[1,7], Tarek Klaylat[1,7], Joseph A Petruccelli[2], Guillaume St-Jean[3], Mohan Radhakrishna[4], Rahul Gawri[1, 5, 6,7], Chan Gao[1, 4, 6].

1. Department of Experimental Surgery, Department of Surgery, McGill University, Montréal, QC, H3G 1A4, Canada

2. Faculty of Medicine, University of Sherbrooke, Sherbrooke, QC, J1H 5N4

3. Department of Pathology and Microbiology, Faculty of Veterinary Medicine, Université de Montréal, QC, J2S 2M2

4. Physical Medicine & Rehabilitation, McGill University, Montréal, QC, H2W 1S4

5. Department of Surgery, McGill University, Montréal, QC, H3A 0G4

6. Department of Medicine, McGill University, Montréal, QC, H3A 0G4

7. Regenerative Orthopaedics and Innovation Laboratory, Division of Orthopaedic Surgery, Department of Surgery, McGill University, Montréal, QC, H3G 1A4, Canada

Abstract:

Heterotopic ossification (HO) is abnormal bone formation in soft tissues and a common complication of spinal cord injury (SCI). In the absence of the adequate knowledge of the pathomechanisms of HO, current prophylactic and therapeutic approaches to SCI-associated HO are limited in their effectiveness and have off-target side effects. Animal models are instrumental for investigation of the etiology of SCI-associated HO; however, no existing animal model recapitulates the polytraumatisms with SCI which is the most common clinical scenario predisposing to SCI-associated HO. Therefore, the goal of this study is to develop a novel and

clinically relevant murine model of SCI-associated HO. Ten-week-old C57BL/6J mice were subjected to spinal cord transection at T9-T10 to induce SCI and concomitant quadriceps crushing and tenotomy to generate musculotendinous injury (MTI) in the Left hindlimb (SCI+MTI) whereas the Right hindlimb remained intact (SCI) (n=17). A cohort of age and sex matched mice underwent MTI in the Left hindlimb (MTI) whereas the Right hindlimb left intact (Control) (n=11). High-resolution micro-CT scans of hindlimbs at 1 and 4 weeks were used to quantify ectopic mineral volumes and femoral bone quality. Undecalcified hindlimbs were then embedded in methyl methacrylate and consecutive 5μm sections were stained with Von Kossa to show mineralized soft tissues, alkaline phosphatase (ALP) for osteoblast activity, and tartrate-resistant acid phosphatase (TRAP) for osteoclast activity. Only SCI+MTI led to ectopic mineral deposit at 1 week and 4 weeks. Quantitative micro-CT analysis showed ectopic mineral volume at 1 week in SCI+MTI (median, Q1 – Q3: 5.67, 2.58 – 8.38) is significantly higher than those of SCI alone (median, Q1 – Q3: 0.324, 0.265 – 0.345, **p=0.0111**) and MTI alone (median, Q1 – Q3: 0.296, 0.241 – 0.378, **p=0.0260**). At 4 weeks, ectopic mineral volume in SCI+MTI (median, Q1 – Q3: 8.72, 6.96 – 17.0) was significantly higher than those of SCI alone (median, Q1 – Q3: 0.26, 0.186 – 0.270, **p<0.0001**) and MTI alone (median, Q1 – Q3: 0.388, 0.346 – 0.434, **p=0.001**). In comparison to non-SCI mice, mice with SCI showed statistically significant thinning of femoral cortical bone (median, Q1 – Q3: 7.43, 7.06 – 7.64 vs. 9.24, 9.01 – 9.56, **p=0.0007**) and reduced trabecular bone (median, Q1 – Q3: 1.93, 1.73 – 2.52, **p=0.0007**) at 4 week whereas the no significant difference was present at 1 week. Histological assessment with Von Kossa and Toluidine Blue staining confirmed ectopic mineral deposit only in the hindlimbs with SCI+MTI at 1 week and formation of ectopic bone with bone marrow at 4 weeks. ALP and TRAP staining corroborated the colocalization of osteoblast and osteoclast activities at loci of ectopic bone formation. Histomorphometric analysis revealed

significant increased osteoblast activity from 1 week to 4 weeks (median, Q1 – Q3: 0.145, 0.112 – 0.181 vs 4.79, 3.78 – 5.70, **p=0.0286**) while the osteoclast activity showed no significant difference between 1 and 4 weeks (median, Q1 – Q3: 0.930, 0.260 – 1.56 vs 0.410, 0.220 – 0.532, p=0.5429). This study represents a novel clinically relevant model of SCI-associated HO to study pathogenic mechanisms and assess novel therapies.

Keywords:

Heterotopic ossification, spinal cord injury, musculotendinous injury, polytrauma, murine model, ectopic mineralization, osteopenia.

1. Introduction:

Heterotopic ossification (HO) is the abnormal formation of bone in soft tissues, such as muscle and tendon (132). HO is a common complication of spinal cord injury (SCI) reported in 15-30% of patients with combined SCI and polytrauma (22, 26, 133, 134). SCI-associated HO affects the muscle and tendon around the large joints, such as hip and knee, and causes pain, joint stiffness, and a worsened quality of life (135). Complete SCI, spasticity, pressure sores and microtrauma due to motor and sensory deficits (135-137) have been linked the occurrence of HO, however, the etiology of SCI-associated HO remains largely unknown. Current prevention modalities like radiation therapy, non-steroidal anti-inflammatory drugs (NSAID) and bisphosphonates are non-specific and limited in relieving chronic pain or preventing recurrence following surgical resection (138). Due to HO's proximity to joints and its ability to entrap nerves and blood vessels, curative surgical resection of HO lesions remains challenging, and the risk of recurrence imposes an additional burden on patients with SCI (139). Therefore, the development of new strategies to allow early diagnosis and effective intervention is required.

Preclinical studies using rodent models have been pivotal in forming a basic understanding of pathogenic mechanisms of HO (13). Few animal models exist for the study of SCI-associated HO. Previously established murine models of SCI-associated HO use intramuscular injections of cardiotoxin and BMP to initiate HO secondary to SCI (105). Although these models are valuable in highlighting the need of commitment injuries for the initiation of the condition (103), administration of BMP or cardiotoxin to induce myocyte death does not recapitulate the clinical scenario of polytrauma. Traumatic SCI are most caused by motor vehicle accident and fall and occurs frequently with concomitant traumatic injuries to other tissues, which influences HO formation. However, this clinical feature of polytrauma with SCI has not been simulated in existing animal models of SCI-associated HO.

To address this issue, we set out to create a reproducible and relevant murine model of SCI-associated HO that mimics polytrauma with SCI. We hypothesized that concomitant SCI and musculotendinous injury (MTI) leads to HO formation. Our findings suggest mouse model of SCI+MTI mimics the common clinical presentation of traumatic SCI with paraplegia. Radiologic and histochemical analyses at 4 weeks post-operative revealed HO characterised by osteoblast, osteoclast, and hematopoietic activities in the injured muscles of SCI+MTI mice.

2. Methods and Materials:

2.1 Animal Use Protocol and Mice

All mice and experimental procedures (AUP 2021-8214) were approved for use by the McGill Facility Animal Care Committee (FACC) in accordance with the policies and guidelines stated by the Canadian Council on Animal Care (CCAC). All mice were acquired from the Jackson Laboratories and housed in the Animal Resources Division at the Research Institute of the McGill

University Health Center (Montreal, QC, Canada). Surgical procedures were performed on 10-week-old female C57BL/6 wild type mice housed under 12-hour light/dark cycles with access to soft food pellets and water ad libitum. Animals were randomly allocated to experimental groups and were thereafter identified by numbered ear tags.

2.2 Surgical Procedures

2.2.1 Spinal Cord Injury

General anesthesia was induced with constant O_2 flow carrying 3% isoflurane. After placing mice prone, a 3 mm posterior incision was made on the skin in the thoracic spine. Once the supraspinous ligaments were located, superficial dorsal muscles were dissected to expose the vertebral column at the T9-T10 level, and a laminectomy was performed with fine-tip forceps to expose the spinal cord. Fine-tipped spring scissors were then used to swiftly perform a complete spinal cord transection (Figure 1.A). A No. 12 surgical blade was then used to ensure lateral segments of the spinal cord were also transected. A muscle reflex can be observed once a SCI is performed. After obtaining adequate hemostasis, the incision was closed with 5-0 vicryl surgical sutures.

2.2.2 Musculotendinous Injury

Immediately following the SCI, a 3mm skin incision was made on the lateral aspect of the LEFT knee. Patella, quadriceps tendon and muscle were located, and a No. 15 blade was then used to form a small plane of dissection in the quadriceps muscle, near the quadriceps tendon, along the long axis of the femur. While holding the musculotendinous tissue in place, a compression was performed for 15 seconds at highest gauge using a surgical clamp, followed by a 2mm quadriceps tenotomy using sharp transection with No. 15 surgical blade (Figure 1.B). The skin incision of

MTI was then closed using surgical staples. The RIGHT hindlimb remained intact as an internal control.

Two cohorts of mice were enrolled in this study to validate this novel mouse model (Figure 1). Cohort 1 was subjected to MTI alone in the left hindlimb (N=12) while the contralateral hindlimb served as a Control, and cohort 2 was subjected to SCI at T9-10 combined with simultaneous MTI (SCI+MTI) in the left hindlimb (N=24) with the contralateral hindlimb serving as the SCI alone condition. Prior to the experimental endpoint, a total of four mice from Cohort 2 were euthanized due to humane endpoints, including urinary blockage (n=1), blood loss (n=1), weight loss >20% (n=1), and recurrent wound dehiscence (n=1). Following micro-CT scanning, a total of four mice were excluded from the post-mortem analysis due to radiological evidence of patellar dislocation or fracture (n=2), or evidence of periosteal reaction (n=2). A total of eleven mice in Cohort 1 (Right: Control; Left: MTI alone) were included in the post-mortem analysis at 1 week (n=6) and 4 weeks (n=5). A total of seventeen mice in Cohort 2 (Right: SCI alone; Left: SCI+MTI) were included in the post-mortem analysis at 1 week (n=7) and 4 weeks (n=10).

2.3 Postoperative Care and Tissue Harvest

Subcutaneous buprenorphine extended release (ER) was administered three hours preoperatively and every 3 days post-operatively at 1mg/kg. All mice received 0.5 mL bolus of subcutaneous saline immediately after surgery and were monitored in a 30º C recovery chamber. For the first post-operative week, mice received 0.5 mL subcutaneous saline twice daily. Soft food and water were placed in petri dishes on the floor of cages to permit easier access for paraplegic mice. Mice bladders were manually expressed twice daily. After euthanizing the mice via cervical dislocation following overdose with isoflurane and CO_2, hindlimbs were then harvested and fixed in 4% paraformaldehyde (PFA).

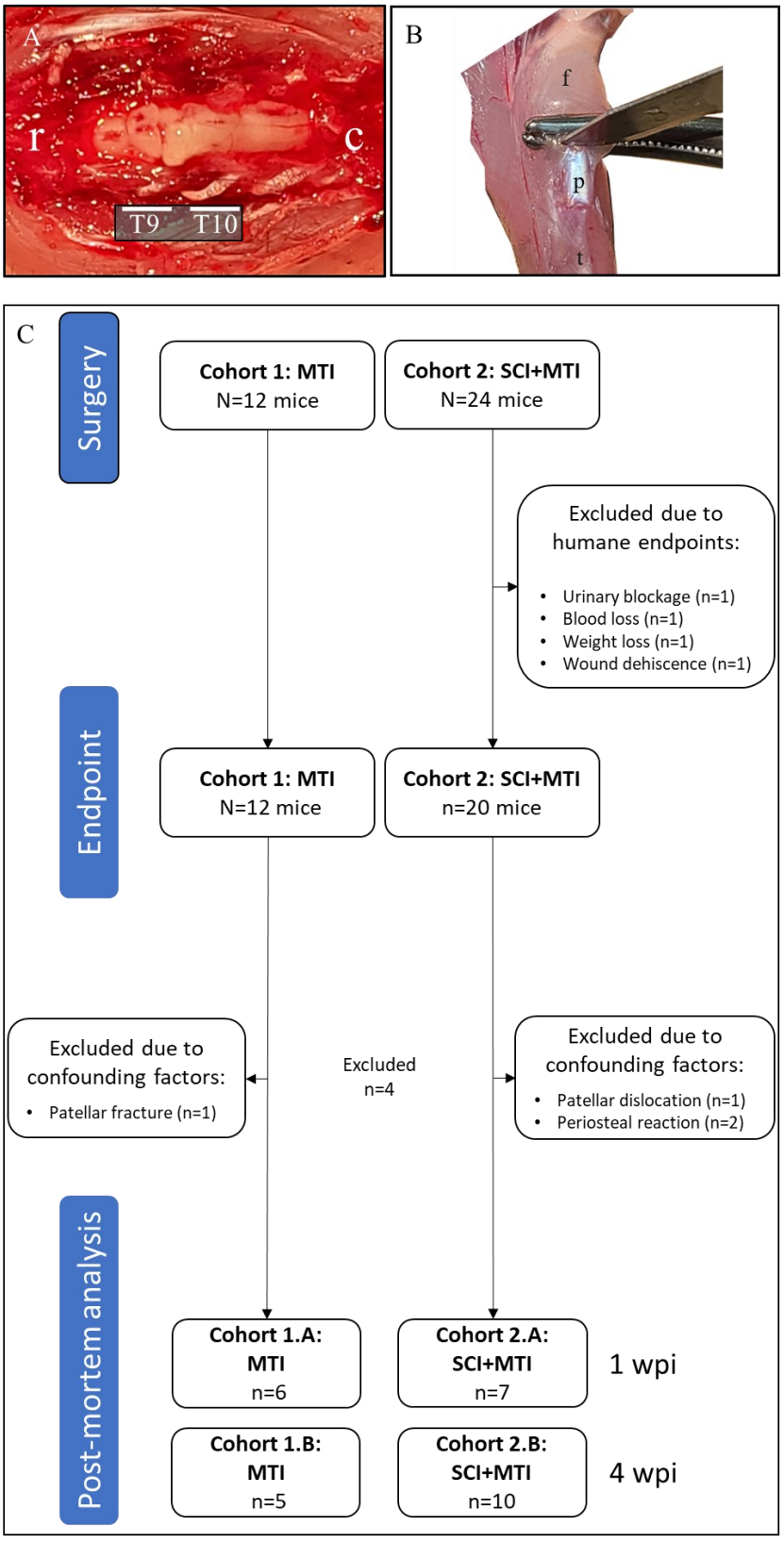

Figure 1. Animal surgery and study design. A. Spinal cord injury (SCI). Spinal cord injury

was induced by spinal cord transection at T9-T10 with spring scissors; r=rostral, c=caudal. **B. Musculotendinous injury (MTI).** MTI was induced by crushing with surgical clamp at the quadriceps tendon for 15 seconds followed by sharp transection with #15 surgical blade; f=femur, p=patella, t=tibia. **C. Illustration of study design.** Cohort 1 was subjected to MTI alone in the left hindlimb (N=12). Cohort 2 was subjected to combined SCI and MTI in the left hindlimb (SCI+MTI) (N=24). Mice from Cohort 2 euthanized due to humane endpoints, including urinary blockage, weight loss >20%, blood loss, and wound dehiscence (n=4). Mice excluded from post-mortem analysis due to patellar dislocation, patellar fracture, and evidence of periosteal reaction (n=4). Mice in Cohort 1 (Right: Control; Left: MTI alone) at 1 week (n=6) and 4 weeks (n=5). And mice in Cohort 2 (Right: SCI alone; Left: SCI+MTI) were included in the post-mortem analysis at 1 week (n=7) and 4 weeks (n=10).

2.4 Micro-computed tomography Scanning and 3D Reconstruction

Following overnight fixation in PFA and two overnight washes in phosphate buffered saline, high resolution micro-computed tomography scans of the hindlimbs were generated with 1172 Skyscan scanner at a spatial resolution of 7µm, voltage of 50 kV, and a current of 200 µA. The field of view of X-ray images was centered on the distal diaphysis and metaphysis of mouse femurs. All 180º scans were performed at medium magnification (2000x1336 pixel resolution), using a rotational step of 0.45°. 3D reconstructions of the hindlimbs were then rendered using NRecon software with appropriate ring artifacts and beam hardening reduction parameters (140).

2.5 Quantitative Assessment of Heterotopic and Orthotopic Bone

CTan software was used to perform the segmentation and quantification of abnormal bone volumes and orthotopic bone architecture. Using a dedicated CTan algorithm, a Region of Interest (ROI) encircling only ectopic mineral and bone spanning 4.2 mm (600 slices) was used for evaluating volume of ectopic mineral deposited in quadriceps muscle (μm^3). Trabecular bone parameters were evaluated after defining an ROI which spans the intramedullary region of the distal metaphysis, starting from the proximal end of the distal physis and ending 1 mm proximally. Cortical bone parameters were assessed after defining an ROI which includes the cortical region of the distal femoral diaphysis spanning 1 mm in length (141).

2.6 Tissue Processing and Embedding

After trimming, tissues were processed in a series of dehydrations, infiltrations, and were embedded in low temperature methyl methacrylate for histological evaluation of bone samples. Blocks were trimmed and consecutive 5 µm sections were collected for histochemical evaluations.

2.7 Histological evaluations

Serial sections underwent an alcohol rehydration series and stained with the respective primary stain, followed by several steps of clearing and washes, and the appropriate counterstaining. Von Kossa and Toluidine Blue staining was used to stain undecalcified samples for mineralized or ossified tissues, Alkaline Phosphatase (ALP) and Nuclear Fast Red to stain osteoblastic activity, and Tartrate-Resistant Acid Phosphatase (TRAP) and Fast Green to stain osteoclastic activity. High resolution images were captured using Zeiss Axioskop 40 (Carl Zeiss,

Toronto, ON, Canada) and histomorphometric analyses were performed in Fiji, Image J2 v.2.11.0. Quantification was performed on regions of interests centered on mineralized and ossified soft tissues from ALP and TRAP-stained sections. Histomorphometric quantification was presented as the percent positively stained area relative to total area of the region of interest and was expressed as % positive of total area.

2.8 Statistical Analyses

Statistical analysis was performed using GraphPad Prism version 9. The Shapiro-Wilk test was used to check for the normal distribution of data points. Kruskal-Wallis test was used to perform non-parametric unpaired statistical analysis between three or more groups. Mann-Whitney U test was used for post hoc analysis. Significance was set at a p value of ≤ 0.05.

3. Results:

3.1 SCI+MTI led to ectopic mineral deposit at the site of MTI

MicroCT 3D reconstructions of mouse hindlimbs showed all hindlimbs with SCI+MTI presenting radiological evidence of ectopic mineralization, whereas no ectopic mineralization or ossification was visualized in Control, MTI alone or SCI alone cohorts at 1- and 4 wpi. Micro-CT imaging of mice subjected to SCI+MTI showed patterns of diffuse mineralization in the injured quadriceps at the site of MTI at 1-week post-injury (wpi) (Figure 2.A). Higher densities with cancellous bone architecture in close proximity to mineralization at the site of MTI at 4 wpi suggestive of ectopic ossification (Figure 2.A).

Quantification of ectopic mineral volume was performed for all groups at both timepoints. At 1 wpi, ectopic mineral volume was significantly increased in the SCI+MTI group (median, Q1 – Q3: 5.67, 2.58 – 8.38) in comparison to the MTI alone group (median, Q1 – Q3: 0.296, 0.241 – 0.378, **p=0.0260**) and the SCI alone group (median, Q1 – Q3: 0.324, 0.265 – 0.345, **p=0.0111**). No statistically significant difference was noted in ectopic mineral volumes between SCI+MTI and Control groups (median, Q1 – Q3: 0.314, 0.273 – 0.354, p=0.0649) at 1 wpi. At 4 wpi, ectopic mineral volumes in the SCI+MTI group (median, Q1 – Q3: 8.72, 6.96 – 17.0) were statistically significant in comparison to the SCI alone group (median, Q1 – Q3: 0.26, 0.186 – 0.270, **p<0.0001**), in comparison to the MTI alone group (median, Q1 – Q3: 0.388, 0.346 – 0.434, **p=0.001**), and in comparison to the Control group (median, Q1 – Q3: 0.313, 0.300 – 0.337, **p=0.001**). There were no statistically significant differences between Control, SCI alone or MTI alone groups at either 1 or 4 wpi (Figure 2.B). Differences in ectopic mineral volumes between 1 wpi and 4 wpi SCI+MTI groups showed an increasing trend; however, no statistical significance was noted (p=0.1135). No statistically significant differences were noted between 1 wpi and 4 wpi timepoints for each of the Control, MTI alone or SCI groups.

A

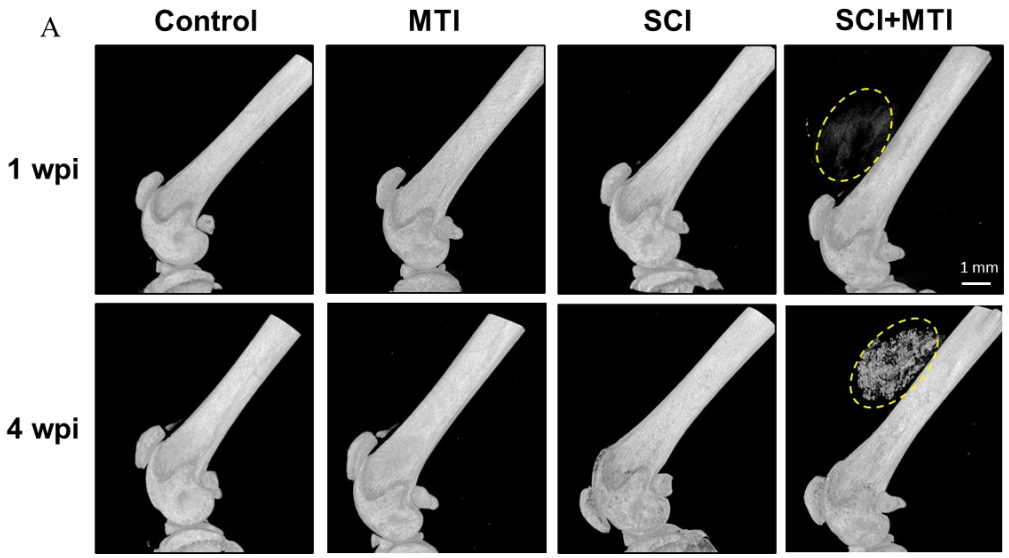
Control
MTI
SCI
SCI+MTI
1 wpi
4 wpi
1 mm

B

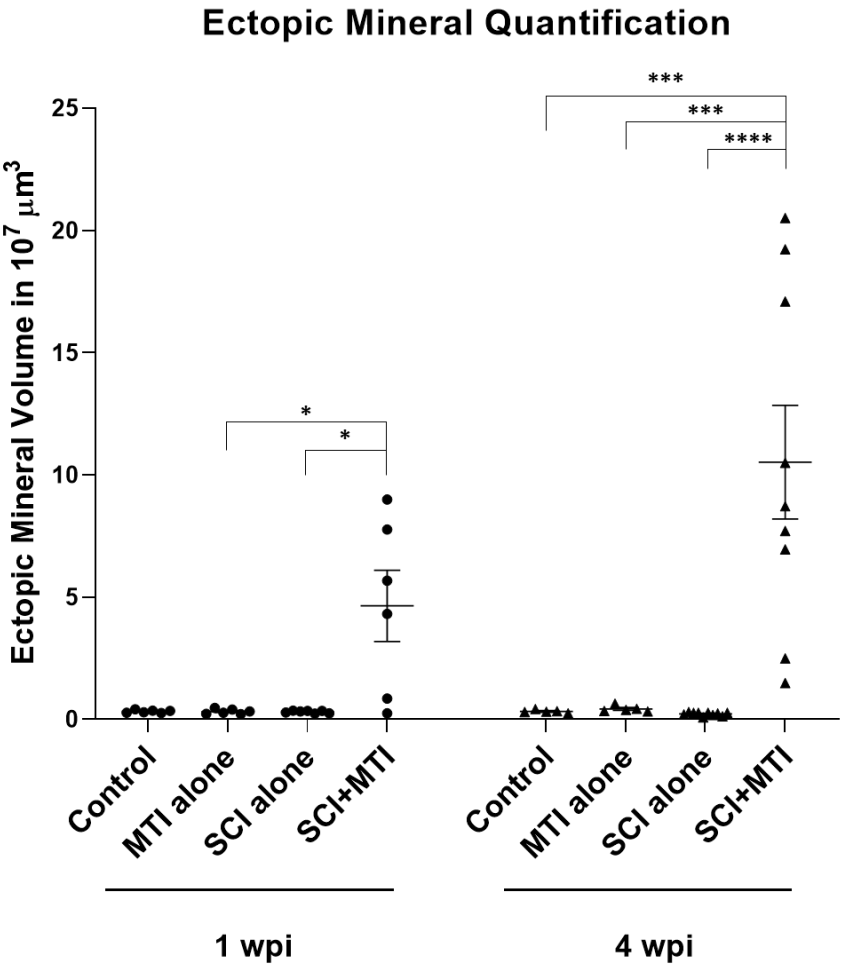
Ectopic Mineral Quantification
Ectopic Mineral Volume in 10^7 μm^3
25
20
15
10
5
0
*
*
***
***
****
Control
MTI alone
SCI alone
SCI+MTI
Control
MTI alone
SCI alone
SCI+MTI
1 wpi
4 wpi

Figure 2. Micro CT analysis of SCI-associated NHO at 1 and 4 weeks. Representative 3D-reconstructed micro CT images of control hindlimbs, MTI alone, SCI alone, and SCI+MTI collected at 1 week and 4 weeks (A). SCI+MTI led to mineralization of quadriceps muscle at 1 week and ossification at 4 weeks whereas no ectopic mineralization was visualized in Control, MTI and SCI alone at either 1 or 4 weeks. Quantification of ectopic mineral showed that the ectopic mineral volume is significantly higher in SCI+MTI at 4 weeks compared to other groups (B) (*$p<0.05$, ***$p<0.001$, ****$p<0.0001$). There is no significant difference found between 1 week and 4 weeks in SCI+MTI, but the tendency of cautious growth of HO was evident. Each symbol represents a separate mouse leg.

3.2 SCI led to cortical thinning and reduced trabecular bone of the femur

3D reconstructions of mouse hindlimbs were segmented for trabecular (Figure 3.B) and cortical (Figure 3.C) analysis to evaluate the effect of SCI, MTI or combined SCI+MTI injuries on orthotopic bone quality. Representative 2D microCT images of mice that underwent single or combined injuries are shown (Figure 3.D). No obvious qualitative difference in gross morphology was visualized between any groups at 1 wpi. At 4 wpi, the thinning of the cortical bone in distal femoral diaphysis and reduced trabecular bone mass in the femoral metaphysis were prominent in mice with SCI in comparison to those without. The ratio of bone volume over total/tissue volume (BV/TV, %) was used to quantify the trabecular bone at the femoral metaphysis (Table 1) and the mean total cross-sectional bone area as a measure of cortical bone thickness at the distal femoral diaphysis (Table 2). Trabecular BV/TV calculated for all groups at 1 and 4 wpi showed no significant differences in trabecular BV/TV were noted between Control, MTI alone, SCI alone and SCI+MTI groups at 1 wpi. At 4 wpi, there was a significant decrease in trabecular bone mass

in the SCI+MTI group (median, Q1 – Q3: 1.74, 1.57 – 2.05) in comparison to MTI alone (median, Q1 – Q3: 5.20, 4.68 – 5.26, p=**0.0007**). SCI alone led to significantly lower BV/TV (median, Q1 – Q3: 1.93, 1.73 – 2.52) in comparison to Control (median, Q1 – Q3: 4.75, 4.46 – 5.76, p=**0.0007**) at 4 wpi, but no statistically significant difference was noted between SCI+MTI and SCI alone (p=0.1431). MTI alone does not alter the trabecular bone mass of distal femur in the presence or absence of SCI.

Trabeculae BV/TV (%)						
	1 week			4 weeks		
	Non-SCI	SCI	P value	Non-SCI	SCI	P value
Right (Control)	7.37 (0.78)	5.41 (2.1)	0.0593	4.75 (1.3)	1.93 (0.79)	**0.0007**
Left (MTI)	6.70 (1.1)	6.30 (2.8)	0.9497	5.20 (0.58)	1.74 (0.48)	**0.0007**
P value	0.1797	0.5737		1.0000	0.1431	

Table 1. Trabecular BV/TV in Control, MTI alone, SCI alone and SCI+ MTI groups at 1 and 4 weeks. SCI led to significantly less trabecular bone at 4 weeks; however, no difference was found between SCI and SCI+MTI. Data presented as median (Interquartile Range).

Cortical bone area (Ct. B.Ar.) calculated for all groups at 1 and 4 wpi (Table 2) revealed no statistically significant difference between any group at 1 wpi. At 4 wpi, Ct. B.Ar. was significantly lower in SCI+MTI group (median, Q1 – Q3: 7.39, 7.00 – 7.62) in comparison to MTI only (median, Q1 – Q3: 9.47, 8.96 – 9.72, **p=0.0007**). At 4 wpi, SCI alone led to significantly lower Ct. B.Ar. (median, Q1 – Q3: 7.43, 7.06 – 7.64) in comparison to Control (median, Q1 – Q3: 9.24, 9.01 – 9.56, **p=0.0007**), but was not statistically significant different from that of SCI+MTI (p=0.9118). MTI alone does not affect the cortical thickness in the presence of absence of SCI.

Cortical Crossectional Area (10^5 µm^2)						
	1 week			4 weeks		
	Non-SCI	SCI	P value	Non-SCI	SCI	P value
Right (Control)	8.33 (0.51)	8.12 (0.57)	0.1812	9.24 (0.55)	7.43 (0.58)	**0.0007**
Left (MTI)	8.29 (0.10)	8.35 (0.51)	1.0000	9.47 (0.76)	7.39 (0.63)	**0.0007**
P value	0.8182	0.2786		0.8413	0.9118	

Table 2. Cortical Cross-sectional Area in Control, MTI alone, SCI alone and SCI+ MTI groups at 1 and 4 weeks. SCI led to significantly thinner cortical bone at 4 weeks; however, no difference was found between SCI and SCI+MTI. Data presented as median (Interquartile Range).

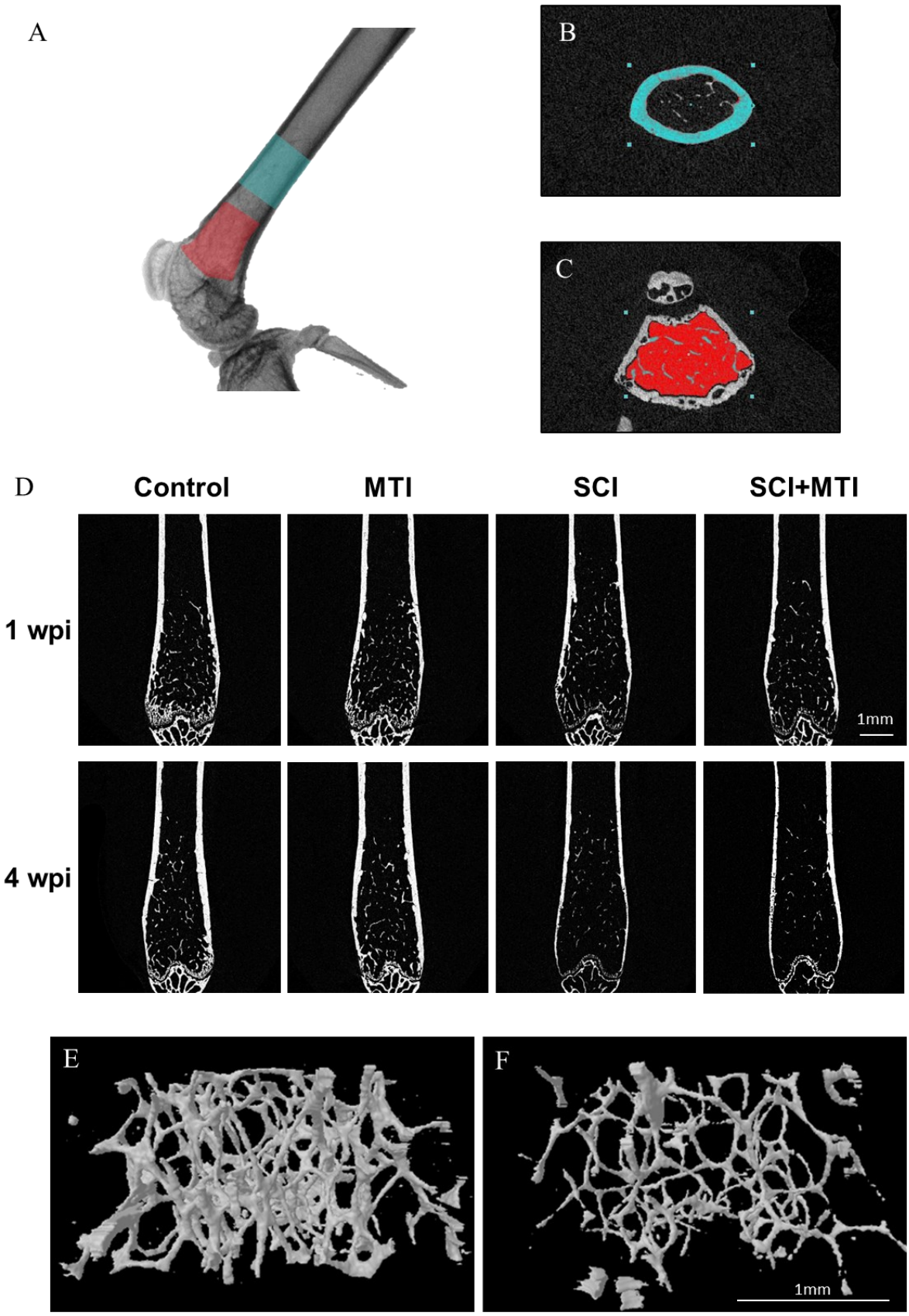
A
B
C
D
Control
MTI
SCI
SCI+MTI
1 wpi
4 wpi
1mm
E
F
1mm

Figure 3. Changes of femoral bone quality in the model of SCI-associated NHO at 1 and 4 weeks. Quantitative micro CT analysis of trabecular bone mass was performed within the volumes of interest (VOI) delineating the metaphyseal region (red area in A) and cortical bone area measurement was performed in the VOI delineating the diaphysis (blue area in A). Distinct regions of interest (ROI) were defined for cortical bone area (B) and trabecular bone mass (C). Representative 2D micro CT images of control hindlimbs, MTI alone, SCI alone, and SCI+MTI collected at 1 week and 4 weeks (D). Representative 3D reconstructions of trabecular bone at distal femurs in non-SCI (H) and SCI (I) mice at 4 weeks. At 4 weeks, the femurs collected from SCI (F2) and SCI+MTI (G2) showed remarkable loss of trabecular bone and thinning of cortical bone.

3.3 SCI+MTI led to active ectopic mineralization and ossification

At 1 wpi, Von Kossa and Toluidine Blue did not show presence of mineral deposits in or near the quadriceps musculotendinous tissue as shown in the representative sections of Control, MTI alone and SCI alone samples (Figure 4.A). MTI samples at 1 wpi showed regions of hypercellularity including multinucleated cells adjacent to myofibers, however no black deposits were observed near this region. Diffuse mineralization of injured quadriceps muscle was present in SCI+MTI samples at 1 wpi (Figure 4.B.A1). At 4 wpi, the healing of quadriceps MTI was visualized in MTI alone group with normal muscle mass and structure present (Figure 4.A). SCI alone led to quadriceps muscle atrophy without HO (Figure 4.A). In SCI+MTI at 4 wpi, the ectopic mineralized tissue consists of acellular mineral deposit (Figure 4.B.B1) and HO lesion characterized by the presence bone marrow and bone matrix lacunae, suggesting active processes of ectopic ossification and hematopoiesis (Figure 4.B.C1).

3.4 SCI+MTI displayed gradual ossification but stagnant remodeling

Consecutive sections were used for ALP and TRAP staining to assess activities of osteoblasts and osteoclasts in the injured quadriceps of SCI+MTI samples. Little to no positive ALP staining was present at the site of MTI at 1 wpi (Figure 4.B.A2). At 4 wpi, strong positive ALP staining, denoted by a blue/purple coloration, was found contouring ectopic mineral deposits (Figure 4.B.B2) and ectopic bone-like tissue (Figure 4.B.C2). TRAP staining was positive at the site of MTI at 1 wpi (Figure 4.B.A3). At 4 wpi, TRAP-positive osteoclasts co-localized with ALP-positive osteoblasts in both regions of ectopic mineralization (Figure 4.B.B3) and ossification (Figure 4.B.C3), suggesting active bone turnover.

Quantification of ALP positive staining in SCI+MTI groups showed a statistically significant increase in the percent ALP positive area at 4 wpi in comparison to 1 wpi (median, Q1 – Q3: 4.79, 3.78 – 5.70 vs. 0.145, 0.113 – 0.181, **p=0.0286**). Quantification of TRAP positive staining in SCI+MTI groups did not show a statistically significant difference between 4 and 1 wpi (median, Q1 – Q3: 0.41, 0.22 – 0.53 vs. 0.93, 0.26 – 1.60, p=0.5429).

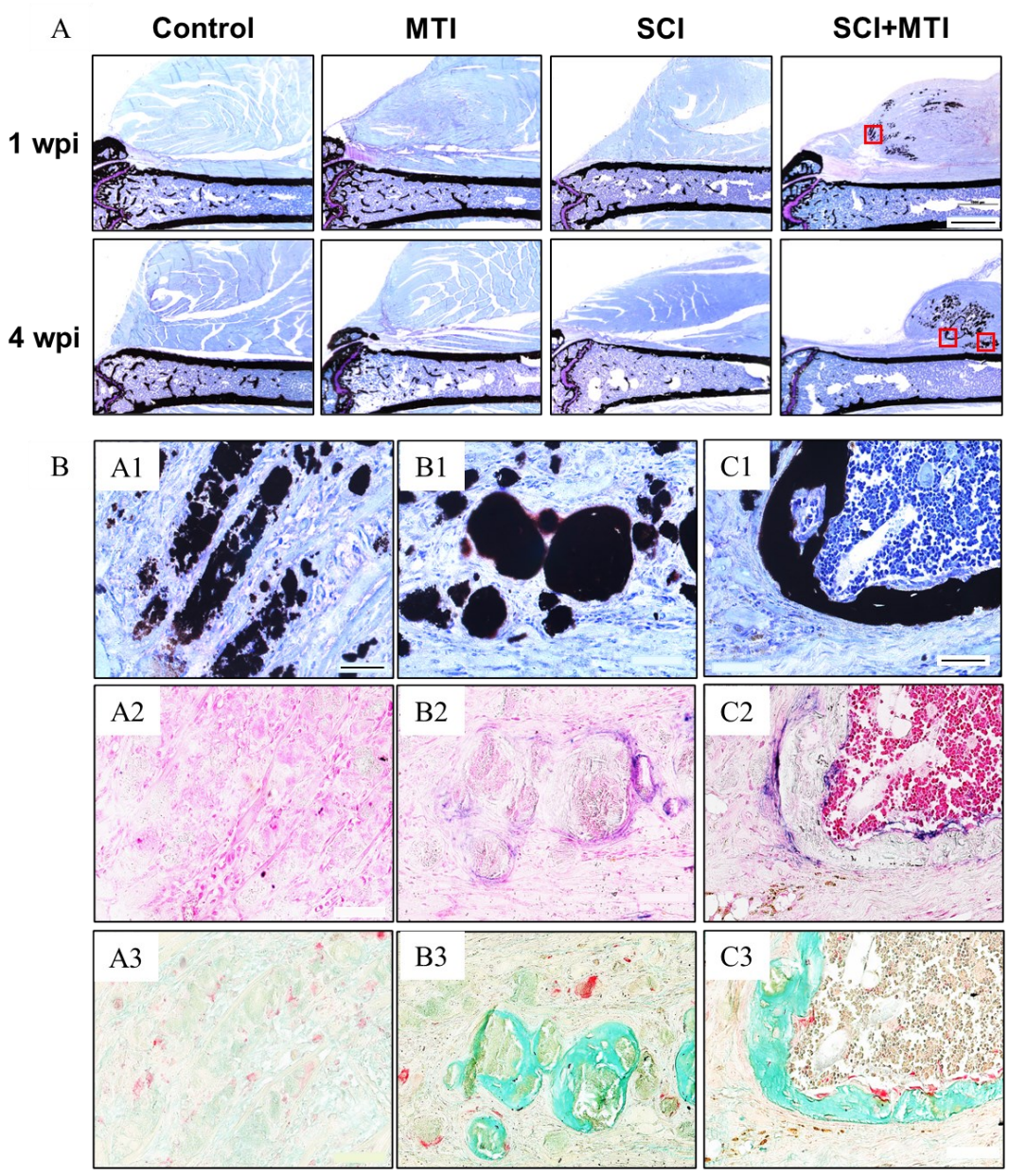
A
Control
MTI
SCI
SCI+MTI
1 wpi
4 wpi
B
A1
B1
C1
A2
B2
C2
A3
B3
C3
C
ALP+ quantification
% ALP
*
SCI+MTI
1 wpi
SCI+MTI
4 wpi
TRAP+ quantification
% TRAP
SCI+MTI
1 wpi
SCI+MTI
4 wpi

Figure 4. Histological analysis of SCI-associated NHO at 1 and 4 weeks. Von Kossa and Toluidine Blue staining of control hindlimbs, MTI alone, SCI alone, and SCI+MTI collected at 1 week and 4 weeks (A); black line denotes 1000 μm. SCI+MTI led to mineralization of quadriceps muscle at 1 week and ossification at 4 weeks whereas no ectopic mineralization was visualized in Control, MTI and SCI lone at either 1 week or 4 weeks. High magnification of the inset in SCI+MTI at 1 week was shown in A1; black line denotes 50 μm. At 1 week, only mineralization was seen in SCI+MTI with little osteoblast but high osteoclast activities as shown by ALP staining and TRAP staining respectively (A1-A3). At 4 weeks, two types of mineralized lesions were seen as defined by 2 insets in SCI+MTI at 4 weeks. One type of mineralized lesion in SCI+MTI at 4 weeks is devoid of bone structure similar to A1 (B1), but it is surrounded by lined with osteoblasts indicated by positive ALP (B2) and osteoclasts indicated by positive (TRAP) (B3). The other type of mineralized lesion (C1) is featured by well-developed bone structure and bone marrow (C1). Similarly, the ectopic bone showed active osteoblast (C2) and osteoclast (C3) activities. Histomorphometry analysis of ALP staining and TRAP staining (C) confirmed significantly higher level of osteoblast but not osteoclast activities in SCI+MTI at 4 weeks which indicate active turnover in the NHO lesion.

4. Discussion:

Neurogenic HO mouse models are crucial to understanding the pathophysiology of SCI-associated neurogenic HO. To develop effective prevention and treatment strategies, it is paramount that mouse models accurately mimic the clinical scenario prior to the onset of the condition. To this end, this study describes the first rodent model of neurogenic HO induced by polytrauma with SCI, which is distinct from previous cardiotoxin or BMP models (105, 126). By

inducing concomitant traumatic spinal cord and quadriceps musculotendinous injuries, we demonstrated that neurogenic HO developed near the knee, as seen in human patients.

As with other mouse models of SCI-associated HO, this mouse model underlined the requirement of combined injuries to the CNS and peripheral soft tissues to consistently induce NHO formation. The onset of ectopic mineralization was denoted at the site of injury as of 1 wpi and proceeded with heterotopic ossifications evident as of 4 wpi. This transition from ectopic mineral to bone substantiates current findings that musculotendinous HO may proceed through the ossification of dystrophic calcification-rich (DC-rich) lesions (85, 142). The combination of DC and HO was reported in human samples of diffuse idiopathic skeletal hyperostosis (DISH) lending further support to the clinical relevance of our model (143). It is reasonable to presume the quadriceps musculotendinous crush injury led to muscle death as seen in blast injuries commonly sustained by military personnel. The dead muscle tissue can suppress the expression of transforming growth factor β-1 (TGF-β1) which leads to DC and enhanced osteoblastic differentiation of the muscle-derived stromal cells (144). The release of mineral into the extracellular matrix (ECM) because of myocyte death may facilitate mineral accumulation at the site of injury (145). The MTI used in our study led to DC and later HO only if combined with concomitant SCI. Severe central nervous system injuries are complicated by multiple systemic changes that have been linked to the development of DC and HO, including elevated level of glucocorticoid (146), enhanced secretion of adrenaline (147), and inhibition of fibrinolysis system (148). DC is mainly composed of hydroxyapatite which has been used as osteoinductive material to drive bone formation (149). Taken together, multiple systemic and local factors following central nervous system and peripheral tissue injuries interact and result in the DC deposit and HO

formation. It remains unknown if altered innervation of paralyzed limbs secondary to SCI affects the development of HO.

Based on our histological findings, TRAP positive cells were present at the injured musculotendinous tissue during the first week after injury and are followed by lining of mineral deposit by osteoblasts, woven bone formation, and ectopic hematopoiesis at 4 weeks. TRAP is expressed not only by osteoclasts but also by macrophages and dendritic cells (150). The macrophages homed at the site of musculotendinous injury can clear tissue debris, remove mineralized ECM, and reverse the HO formation (151) (152). In the context of SCI, macrophage-derived oncostatin M (OSM) was shown to enhance HO formation in a mouse model of SCI-associated HO (153). Infiltrating monocytes/macrophages undergo osteoclast differentiation under the stimulation of macrophage colony stimulating factor (M-CSF) and receptor activator of nuclear factor-kB ligand (RANKL) (154). Osteoclasts and pre-osteoclasts play pivotal roles in the formation of bone marrow cavity, migration of hematopoietic cells, regulation of osteoblast differentiation, and bone homeostasis and remodeling (155). At 4 wpi, colocalization of osteoblasts and osteoclast-like cells as indicated by high ALP and TRAP activities suggested active bone formation and remodeling occurred at the site of injury. Bone marrow cavities formed within this newly formed woven bone and were filled with various cell types suggesting hematopoiesis. The relationship between monocyte infiltration, osteoclastogenesis, and DC/HO in the context of SCI is yet to be elucidated.

In addition to providing a clinically relevant model for HO following SCI, this model also recapitulates SCI-associated bone loss, as we confirm distal femoral cortical thinning and reduced trabecular bone density occurring within the same period. Additionally, multilocular cells resembling adipocytes were observed near the HO lesion, which were not present in singly injured

or uninjured mice at 4 weeks. This may suggest that the involved stem cells have both adipogenic and osteoblastic potential. Yet the origin of these stem cells, whether from tendon, muscle or from circulation, is yet to be determined.

In summary, this mouse model of SCI-associated HO not only recapitulates the progression of DC-rich lesions into mature bone, but also temporally substantiates the presence, close association and colocalization of osteoclasts and osteoblasts at the site of injury. In addition to permitting the study of concomitant SCI-induced osteopenia, this model showcases the induction of novel ectopic bone formation, hematopoiesis, faulty muscle/tendon regeneration, and facilitates the accurate study of a SCI-associated dysregulated neuronal responses on tissue regeneration and homeostasis. Studies are underway to elucidate neurogenic, angiogenic and brown adipogenic capacities near the NHO lesion and their contribution to the initiation, maturation, and maintenance of abnormal bone in this novel mouse model.

CHAPTER 4: DISCUSSION AND CONCLUSIONS

1. Discussion and Future Directions:

The model developed in my thesis work represents the first mouse model of polytrauma with SCI-associated HO, which was induced by spinal cord transection at T9-T10 combined with a quadriceps musculotendinous crush injury followed by tenotomy. Our model is novel compared to other neurogenic HO mouse models, as previous SCI+BMP and TBI+fracture+muscle crush models reported single injuries leading to trauma-associated HO in a small proportion of mice. In our model, HO developed only when peripheral injuries were combined with SCI. Moreover, other debilitating sequelae of SCI are recapitulated in this model, as we showed trabecular and cortical abnormalities following SCI in skeletally immature genetically unmodified mice. Furthermore, we also provided the first findings suggesting that MTI did not significantly contribute to deteriorating native bone quality induced by SCI. Moreover, our histological findings substantiate those of previous studies suggesting the development of HO from DC-rich lesions in SCI-associated HO (105).

Additionally, we highlighted the presence and close association of TRAP positive multinucleated cells near abnormal deposits at 1 wpi, suggesting an important role for osteoclast-like cells at the site of soft tissue injury in the context of SCI. On the other hand, osteoblasts were not present at 1 wpi and osteoblast-driven mineral accumulation was not observed via ALP staining at this timepoint. Our histological findings may warrant the investigation of antiresorptive agents, such as bisphosphonates, as an early prevention modality for HO. However, administration of non-specific anti-resorptive agents may lead to decreased osteoclast activity not only at the site of injury, but also at off-target sites. This could also lead to the targeting of over-active osteoclasts in the native femur undergoing mechanical unloading following SCI (156). As osteopenia is also a feature of this SCI model, bisphosphonates could be useful to target the involvement of

osteoclasts in early HO phases and their potential role in SCI-induced osteopenia. Nevertheless, further studies are required to confirm the integral role of osteoclasts in early HO stages and their possible involvement in SCI-induced osteopenia. In contrast to a mechanical explanation for SCI-induced osteopenia, other studies have suggested the biological role of SCI-associated dysregulated neuronal responses in the abnormal maintenance of femoral bone mineral density (157, 158). In either case, this mouse model provides a useful platform to assess both mechanical and biological hypotheses and prospective treatments.

The role of dysregulated neuronal responses following SCI on NHO initiation and progression is largely unknown. Several studies have alluded to different mediators of HO following CNS injury. Patients with spinal cord injury have varying serum levels of humoral factors which have been described in experimental models as pro-osteogenic. Increased cytokine levels of TGF-β and interleukins have been particularly linked with increased activity of osteoblasts following SCI in experimental models (159-161). Furthermore, heterotopic bone seems to be densely innervated in several animal models of HO. This abnormal innervation of peripheral injury sites was positively correlated with heterotopic bone growth and the cooccurring differentiation of resident stem cells was shown to be closely involved in the initiation of HO. Moreover, one study showed that abrogation of innervation following the induction of HO decreased abnormal bone volumes (162). Another study suggested that peripheral nerves could harbor stem cells with osteogenic potential near the site of HO (98). The direct contribution of these stem cells to HO formation was observed in inducible models of the condition, however the involvement of these stem cells from peripheral nerves in NHO initiation is yet to be confirmed. Following trauma to soft tissues, peripheral nerve fibers release neurotrophic peptides, like Nerve Growth Factor, and neurotransmitters such as Substance P and Calcitonin gene-related peptide

(CGRP) (163, 164), which have been linked to the cascade of events in the onset of HO (162, 165). Administration of these neuroinflammatory substances in soft tissue was observed to accelerate HO in vivo and in vitro (166). Nevertheless, the integral role of abnormal nerve responses secondary to SCI in NHO progression remains elusive. To investigate how SCI may permit NHO, this mouse model may serve as a useful tool to study the contributions of these potential neurological mediators of NHO initiation and progression. As a future direction for this model, we may characterize in further detail the neurogenesis and axonal invasion which accompanies the growth of HO lesions. With this mouse model, elucidating the types of nerve fibers which have grown/regenerated at sites of peripheral injuries, as well as the interactions of associated neurotrophic factors and secreted neuropeptides, may enhance our understanding of NHO and more broadly the intricacies of nerve and bone interplay. Furthermore, novel bone requires adequate blood supply for its maintenance and growth, and investigating the cooccurrence of neurogenic and angiogenic capacities near HO lesions could elucidate further on the microenvironmental changes which permit NHO progression. While a spinal cord transection seems sufficient to induce NHO formation in our model, it is warranted to investigate the severity of SCI, its implications on sensory and motor function, and ultimately the final disease state in this mouse model. To refine this model, the severity of SCI and its contribution to HO initiation and progression is under investigation through the use of spinal cord contusions (SCC) versus spinal cord transection (SCT). Finally, rather than inducing hyperactivity in signaling pathways to induce HO, we aim to employ this model to investigate their respective pathogenic contributions to HO initiation and progression. We propose several future directions for this model, such as investigating unhindered BMP, Wnt, and GNAS-related signaling pathways, and microenvironmental triggers, such as osteoimmunological mediators and dysregulated neuronal

responses, which create an osteoinductive environment for progenitors to differentiate down the osteoblastic lineage.

Considering the novelty of this study, certain limitations arose when establishing this method of studying SCI-associated HO. While SCI by complete transection is rarely observed in this polytraumatic scenario (167), its use is beneficial to recapitulate severe SCI-associated sequelae such as HO, osteopenia, bladder dysfunction, and neuropathic pain behavior. While SCI is more common in men than in women (168, 169), SCI-associated bladder sequelae in male mice is less manageable due to sex-specific anatomical differences that make manual bladder expression less feasible (170). We therefore opted for the use of female mice to mitigate the negative effects not only on animal well-being, but also on the sustainability of this mouse model. While higher cervical and thoracic SCIs are more likely to result in HO (12), we settled for a less severe lower thoracic transection to maintain HO incidence, yet mitigate possible impingements to animal welfare. Although SCI-associated HO of the hip is more common than that of the knee (132), we opted to investigating the understudied involvement of the knee in this condition. To maximize the replicability and utility of this model, we described our study design and detailed the confounding factors which may arise. Although these surgeries are highly invasive, we detailed how complications can be managed post-operatively to maximize the sustainability of this mouse model.

In our study, the right hindlimbs remained intact to serve as internal controls for MTI in mice with no SCI and SCI+MTI in SCI mice. This experimental design reduces the potential for confounding and the number of animals. Furthermore, considering that our model employs quadruped mice as subjects to mimic the clinical scenario of biped humans, mice may experience differences in mechanical loading and unloading in hindlimbs following SCI in comparison to

humans (171). Especially since immobility in humans is considered a risk factor for developing SCI-associated HO, this poses interesting questions whether these differences across the mouse skeleton may impact NHO onset and progression. In this model, we employed ten-week-old mice to recreate NHO. Humans reach skeletal maturity around late adolescence, while mice reach skeletal maturity around 15 weeks (172). To approximate the mean age of development of NHO in humans, which is close to 20-30 years old, we opted to use genetically unmodified wild-type mice which are nearing skeletal maturity.

2. Conclusion:

In this study, we tested whether a traumatic musculotendinous injury combined with SCI in mice leads to SCI-associated HO as seen in human patients. To this end, we developed a surgical protocol to reliably and reproducibly induce concomitant SCI and musculotendinous injury in genetically unmodified mice. Moreover, we characterized the formation of ectopic mineral deposit and orthotopic bone alterations following polytrauma *in vivo* through radiological and histological assessments. *In vivo* characterization showed that this surgical protocol induced ectopic mineralization and ossification in mice and recapitulated other SCI-associated sequelae observed in patients with SCI. Our findings show that we developed and established the first preclinical model of polytrauma with SCI-associated HO. The development of this model allows mechanism studies of HO regarding stem cell niches, osteoimmunological microenvironments and systemic dysregulations which underlie this condition. This mouse model shows promise in developing and testing novel diagnostic markers and effective therapeutic strategies for patients with SCI-associated HO.

REFERENCES

1. Connor JM, Evans DA. Genetic aspects of fibrodysplasia ossificans progressiva. J Med Genet. 1982;19(1):35-9.

2. Lipscomb AB, Thomas ED, Johnston RK. Treatment of myositis ossificans traumatica in athletes. The American Journal of Sports Medicine. 1976;4(3):111-20.

3. Royce PM, Steinmann B. Connective tissue and its heritable disorders: molecular, genetic, and medical aspects: John Wiley & Sons; 2003.

4. Kaplan FS, Craver R, MacEwen GD, Gannon FH, Finkel G, Hahn G, et al. Progressive osseous heteroplasia: a distinct developmental disorder of heterotopic ossification. Two new case reports and follow-up of three previously reported cases. J Bone Joint Surg Am. 1994;76(3):425-36.

5. Weinstein LS, Collins MT, Spiegel AM. Chapter 27 - Gsα, Pseudohypoparathyroidism, Fibrous Dysplasia, and McCune–Albright Syndrome. In: Thakker RV, Whyte MP, Eisman JA, Igarashi T, editors. Genetics of Bone Biology and Skeletal Disease. San Diego: Academic Press; 2013. p. 425-40.

6. Shore EM, Ahn J, de Beur SJ, Li M, Xu M, Gardner RJM, et al. Paternally Inherited Inactivating Mutations of the GNAS1 Gene in Progressive Osseous Heteroplasia. New England Journal of Medicine. 2002;346(2):99-106.

7. Shore EM, Xu M, Feldman GJ, Fenstermacher DA, Cho T-J, Choi IH, et al. A recurrent mutation in the BMP type I receptor ACVR1 causes inherited and sporadic fibrodysplasia ossificans progressiva. Nature Genetics. 2006;38(5):525-7.

8. Fischer JA, Egert F, Werder E, Born W. An inherited mutation associated with functional deficiency of the alpha-subunit of the guanine nucleotide-binding protein Gs in pseudo- and pseudopseudohypoparathyroidism. J Clin Endocrinol Metab. 1998;83(3):935-8.

9. Ceillier A, editor Para-ostéoarthropathies des paraplégiques par lésions medullaries: Étude clinique et radiographique. Annales de Médecine; 1918.

10. Sumiyoshi K, Tsuneyoshi M, Enjoji M. Myositis ossificans. A clinicopathologic study of 21 cases. Acta Pathol Jpn. 1985;35(5):1109-22.

11. Garland DE. A clinical perspective on common forms of acquired heterotopic ossification. Clinical Orthopaedics and Related Research (1976-2007). 1991;263:13-29.

12. Wittenberg RH, Peschke U, Bötel U. Heterotopic ossification after spinal cord injury. Epidemiology and risk factors. J Bone Joint Surg Br. 1992;74(2):215-8.

13. Hwang CD, Pagani CA, Nunez JH, Cherief M, Qin Q, Gomez-Salazar M, et al. Contemporary perspectives on heterotopic ossification. JCI Insight. 2022;7(14).

14. Gurcay E, Ozturk EA, Erdem T, Gurcay AG, Cakci A. Heterotopic ossification as rare complication of hemiplegia following stroke: Two cases. Brain Injury. 2013;27(13-14):1727-31.

15. Brooker AF, Bowerman JW, Robinson RA, Riley LH, Jr. Ectopic ossification following total hip replacement. Incidence and a method of classification. The Journal of bone and joint surgery American volume. 1973;55(8):1629-32.

16. Engber WD, Reynen P. Post-burn heterotopic ossification at the elbow. Iowa Orthop J. 1994;14:38-41.

17. Moore KD, Goss K, Anglen JO. Indomethacin versus radiation therapy for prophylaxis against heterotopic ossification in acetabular fractures: a randomised, prospective study. J Bone Joint Surg Br. 1998;80(2):259-63.

18. Forsberg JA, Pepek JM, Wagner S, Wilson K, Flint J, Andersen RC, et al. Heterotopic ossification in high-energy wartime extremity injuries: prevalence and risk factors. J Bone Joint Surg Am. 2009;91(5):1084-91.

19. Subedi N, Heire P, Parmer V, Beardmore S, Oh C, Jepson F, et al. Multimodality imaging review of the post-amputation stump pain. Br J Radiol. 2016;89(1068):20160572.

20. Banovac K, Williams JM, Patrick LD, Haniff YM. Prevention of heterotopic ossification after spinal cord injury with indomethacin. Spinal Cord. 2001;39(7):370-4.

21. Banovac K, Gonzalez F. Evaluation and management of heterotopic ossification in patients with spinal cord injury. Spinal Cord. 1997;35(3):158-62.

22. Teasell RW, Mehta S, Aubut JL, Ashe MC, Sequeira K, Macaluso S, et al. A systematic review of the therapeutic interventions for heterotopic ossification after spinal cord injury. Spinal Cord. 2010;48(7):512-21.

23. Sundaram M, Wang LL, Rotman M, Howard R, Saboeiro AP. Florid reactive periostitis and bizarre parosteal osteochondromatous proliferation: pre-biopsy imaging evolution, treatment and outcome. Skeletal Radiology. 2001;30(4):192-8.

24. Winkler S, Wagner F, Weber M, Matussek J, Craiovan B, Heers G, et al. Current therapeutic strategies of heterotopic ossification--a survey amongst orthopaedic and trauma departments in Germany. BMC Musculoskelet Disord. 2015;16:313.

25. Brouwer KM, Lindenhovius AL, de Witte PB, Jupiter JB, Ring D. Resection of heterotopic ossification of the elbow: a comparison of ankylosis and partial restriction. J Hand Surg Am. 2010;35(7):1115-9.

26. Banovac K, Williams JM, Patrick LD, Haniff YM. Prevention of heterotopic ossification after spinal cord injury with indomethacin. Spinal Cord. 2001;39(7):370-4.

27. Milgram J. Myositis ossificans and heterotopic bone. Radiologic and histologic pathology of nontumorous diseases of bones and joints Illinois: Northbrook Publishing. 1990;454.

28. Kluger G, Kochs A, Holthausen H. Heterotopic ossification in childhood and adolescence. Journal of Child Neurology. 2000;15(6):406-13.

29. Kitterman JA, Kantanie S, Rocke DM, Kaplan FS. Iatrogenic Harm Caused by Diagnostic Errors in Fibrodysplasia Ossificans Progressiva. Pediatrics. 2005;116(5):e654-e61.

30. Anderson ME, DuBois SG, Gebhardt MC. 89 - Sarcomas of Bone. In: Niederhuber JE, Armitage JO, Kastan MB, Doroshow JH, Tepper JE, editors. Abeloff's Clinical Oncology (Sixth Edition). Philadelphia: Elsevier; 2020. p. 1604-54.e8.

31. Kransdorf MJ, Meis JM. From the archives of the AFIP. Extraskeletal osseous and cartilaginous tumors of the extremities. Radiographics. 1993;13(4):853-84.

32. Ateschrang A, Gratzer C, Weise K. Incidence and effect of calcifications after open-augmented Achilles tendon repair. Archives of Orthopaedic and Trauma Surgery. 2008;128(10):1087-92.

33. Luczyńska E, Kasperkiewicz H, Domalik A, Cwierz A, Bobek-Billewicz B. Myositis ossificans mimicking sarcoma, the importance of diagnostic imaging - case report. Pol J Radiol. 2014;79:228-32.

34. Tyler P, Saifuddin A. The imaging of myositis ossificans. Semin Musculoskelet Radiol. 2010;14(2):201-16.

35. Enzinger F, Enzinger WS. Weiss's soft tissue tumors. Shock. 2008;30(6):754.

36. Gonda K, Nakaoka T, Yoshimura K, Otawara-Hamamoto Y, Harrii K. Heterotopic ossification of degenerating rat skeletal muscle induced by adenovirus-mediated transfer of bone morphogenetic protein-2 gene. J Bone Miner Res. 2000;15(6):1056-65.

37. Kawao N, Tamura Y, Okumoto K, Yano M, Okada K, Matsuo O, et al. Plasminogen Plays a Crucial Role in Bone Repair. Journal of Bone and Mineral Research. 2013;28(7):1561-74.

38. Hoch B, Montag A. Reactive bone lesions mimicking neoplasms. Seminars in Diagnostic Pathology. 2011;28(1):102-12.

39. Pavey GJ, Polfer EM, Nappo KE, Tintle SM, Forsberg JA, Potter BK. What Risk Factors Predict Recurrence of Heterotopic Ossification After Excision in Combat-related Amputations? Clin Orthop Relat Res. 2015;473(9):2814-24.

40. Garland DE, Hanscom DA, Keenan MA, Smith C, Moore T. Resection of heterotopic ossification in the adult with head trauma. JBJS. 1985;67(8):1261-9.

41. STOVER SL, NIEMANN KMW, TULLOSS JR. Experience With Surgical Resection of Heterotopic Bone in Spinal Cord Injury Patients. Clinical Orthopaedics and Related Research®. 1991;263:71-7.

42. Coons D, Godleski M. Range of motion exercises in the setting of burn-associated heterotopic ossification at the elbow: case series and discussion. Burns. 2013;39(4):e34-8.

43. Holavanahalli RK, Helm PA, Parry IS, Dolezal CA, Greenhalgh DG. Select practices in management and rehabilitation of burns: a survey report. J Burn Care Res. 2011;32(2):210-23.

44. Ritter MA, Sieber JM. Prophylactic indomethacin for the prevention of heterotopic bone formation following total hip arthroplasty. Clin Orthop Relat Res. 1985(196):217-25.

45. Kienapfel H, Koller M, Wüst A, Sprey C, Merte H, Engenhart-Cabillic R, et al. Prevention of heterotopic bone formation after total hip arthroplasty: a prospective randomised study comparing postoperative radiation therapy with indomethacin medication. Arch Orthop Trauma Surg. 1999;119(5-6):296-302.

46. Oni JK, Pinero JR, Saltzman BM, Jaffe FF. Effect of a selective COX-2 inhibitor, celecoxib, on heterotopic ossification after total hip arthroplasty: a case-controlled study. Hip Int. 2014;24(3):256-62.

47. Banovac K, Williams JM, Patrick LD, Levi A. Prevention of heterotopic ossification after spinal cord injury with COX-2 selective inhibitor (rofecoxib). Spinal Cord. 2004;42(12):707-10.

48. Beckmann JT, Wylie JD, Potter MQ, Maak TG, Greene TH, Aoki SK. Effect of Naproxen Prophylaxis on Heterotopic Ossification Following Hip Arthroscopy: A Double-Blind Randomized Placebo-Controlled Trial. J Bone Joint Surg Am. 2015;97(24):2032-7.

49. Subbarao JV, Nemchausky BA, Gratzer M. Resection of heterotopic ossification and Didronel therapy--regaining wheelchair independence in the spinal cord injured patient. J Am Paraplegia Soc. 1987;10(1):3-7.

50. Banovac K. The effect of etidronate on late development of heterotopic ossification after spinal cord injury. J Spinal Cord Med. 2000;23(1):40-4.

51. Thomas BJ, Amstutz HC. Results of the administration of diphosphonate for the prevention of heterotopic ossification after total hip arthroplasty. J Bone Joint Surg Am. 1985;67(3):400-3.

52. Shafer DM, Bay C, Caruso DM, Foster KN. The use of eidronate disodium in the prevention of heterotopic ossification in burn patients. Burns. 2008;34(3):355-60.

53. Nollen AJ. Effects of ethylhydroxydiphosphonate (EHDP) on heterotopic ossification. Acta Orthop Scand. 1986;57(4):358-61.

54. Seegenschmiedt MH, Makoski HB, Micke O. Radiation prophylaxis for heterotopic ossification about the hip joint--a multicenter study. Int J Radiat Oncol Biol Phys. 2001;51(3):756-65.

55. Mishra MV, Austin L, Parvizi J, Ramsey M, Showalter TN. Safety and efficacy of radiation therapy as secondary prophylaxis for heterotopic ossification of non-hip joints. J Med Imaging Radiat Oncol. 2011;55(3):333-6.

56. Müseler AC, Grasmücke D, Jansen O, Aach M, Meindl R, Schildhauer TA, et al. In-hospital outcomes following single-dose radiation therapy in the treatment of heterotopic ossification of the hip following spinal cord injury-an analysis of 444 cases. Spinal Cord. 2017;55(3):244-6.

57. Hamid N, Ashraf N, Bosse MJ, Connor PM, Kellam JF, Sims SH, et al. Radiation therapy for heterotopic ossification prophylaxis acutely after elbow trauma: a prospective randomized study. J Bone Joint Surg Am. 2010;92(11):2032-8.

58. Li Q, Jiang Q, Uitto J. Ectopic mineralization disorders of the extracellular matrix of connective tissue: molecular genetics and pathomechanisms of aberrant calcification. Matrix Biol. 2014;33:23-8.

59. Budoff MJ, Shaw LJ, Liu ST, Weinstein SR, Mosler TP, Tseng PH, et al. Long-term prognosis associated with coronary calcification: observations from a registry of 25,253 patients. J Am Coll Cardiol. 2007;49(18):1860-70.

60. Boulman N, Slobodin G, Rozenbaum M, Rosner I. Calcinosis in rheumatic diseases. Semin Arthritis Rheum. 2005;34(6):805-12.

61. Pfendner EG, Vanakker OM, Terry SF, Vourthis S, McAndrew PE, McClain MR, et al. Mutation detection in the ABCC6 gene and genotype-phenotype analysis in a large international case series affected by pseudoxanthoma elasticum. J Med Genet. 2007;44(10):621-8.

62. Vanakker OM, Martin L, Schurgers LJ, Quaglino D, Costrop L, Vermeer C, et al. Low serum vitamin K in PXE results in defective carboxylation of mineralization inhibitors similar to the GGCX mutations in the PXE-like syndrome. Lab Invest. 2010;90(6):895-905.

63. Jiang Q, Li Q, Grand-Pierre AE, Schurgers LJ, Uitto J. Administration of vitamin K does not counteract the ectopic mineralization of connective tissues in Abcc6 (-/-) mice, a model for pseudoxanthoma elasticum. Cell Cycle. 2011;10(4):701-7.

64. Kim S, Tran TXM, Song H, Park B. Microcalcifications, mammographic breast density, and risk of breast cancer: a cohort study. Breast Cancer Res. 2022;24(1):96.

65. Menck K, Scharf C, Bleckmann A, Dyck L, Rost U, Wenzel D, et al. Tumor-derived microvesicles mediate human breast cancer invasion through differentially glycosylated EMMPRIN. Journal of Molecular Cell Biology. 2014;7(2):143-53.

66. Zhang J-H, Wang J, Tang J, Barnett B, Dickson J, Hahsimoto N, et al. Bone sialoprotein promotes bone metastasis of a non-bone-seeking clone of human breast cancer cells. Anticancer research. 2004;24(3A):1361-8.

67. Leal-Orta E, Ramirez-Ricardo J, Garcia-Hernandez A, Cortes-Reynosa P, Salazar EP. Extracellular vesicles from MDA-MB-231 breast cancer cells stimulated with insulin-like growth factor 1 mediate an epithelial-mesenchymal transition process in MCF10A mammary epithelial cells. J Cell Commun Signal. 2022;16(4):531-46.

68. Bellahcène A, Castronovo V. Increased expression of osteonectin and osteopontin, two bone matrix proteins, in human breast cancer. Am J Pathol. 1995;146(1):95-100.

69. Barnes GL, Javed A, Waller SM, Kamal MH, Hebert KE, Hassan MQ, et al. Osteoblast-related transcription factors Runx2 (Cbfa1/AML3) and MSX2 mediate the expression of bone sialoprotein in human metastatic breast cancer cells. Cancer Res. 2003;63(10):2631-7.

70. Sarvari BK, Sankara Mahadev D, Rupa S, Mastan SA. Detection of Bone Metastases in Breast Cancer (BC) Patients by Serum Tartrate-Resistant Acid Phosphatase 5b (TRACP 5b), a Bone Resorption Marker and Serum Alkaline Phosphatase (ALP), a Bone Formation Marker, in Lieu of Whole Body Skeletal Scintigraphy with Technetium99m MDP. Indian J Clin Biochem. 2015;30(1):66-71.

71. Korpela J, Tiitinen SL, Hiekkanen H, Halleen JM, Selander KS, Väänänen HK, et al. Serum TRACP 5b and ICTP as markers of bone metastases in breast cancer. Anticancer Res. 2006;26(4b):3127-32.

72. Usoro NI, Omabbe MC, Usoro CA, Nsonwu A. Calcium, inorganic phosphates, alkaline and acid phosphatase activities in breast cancer patients in Calabar, Nigeria. Afr Health Sci. 2010;10(1):9-13.

73. Guerreiro S, Monteiro R, Martins MJ, Calhau C, Azevedo I, Soares R. Distinct modulation of alkaline phosphatase isoenzymes by 17beta-estradiol and xanthohumol in breast cancer MCF-7 cells. Clin Biochem. 2007;40(3-4):268-73.

74. Ranganathan K, Loder S, Agarwal S, Wong VW, Forsberg J, Davis TA, et al. Heterotopic Ossification: Basic-Science Principles and Clinical Correlates. J Bone Joint Surg Am. 2015;97(13):1101-11.

75. Urist MR, Nakagawa M, Nakata N, Nogami H. Experimental myositis ossificans: cartilage and bone formation in muscle in response to a diffusible bone matrix-derived morphogen. Arch Pathol Lab Med. 1978;102(6):312-6.

76. Kan C, Yang J, Na D, Xu Y, Yang B, Zhao H, et al. Inhibition of immune checkpoints prevents injury-induced heterotopic ossification. Bone Res. 2019;7:33.

77. Cocks M, Mohan A, Meyers CA, Ding C, Levi B, McCarthy E, et al. Vascular patterning in human heterotopic ossification. Hum Pathol. 2017;63:165-70.

78. Hall BK, Miyake T. The membranous skeleton: the role of cell condensations in vertebrate skeletogenesis. Anat Embryol (Berl). 1992;186(2):107-24.

79. Ducy P, Zhang R, Geoffroy V, Ridall AL, Karsenty G. Osf2/Cbfa1: a transcriptional activator of osteoblast differentiation. Cell. 1997;89(5):747-54.

80. Storm EE, Huynh TV, Copeland NG, Jenkins NA, Kingsley DM, Lee SJ. Limb alterations in brachypodism mice due to mutations in a new member of the TGF beta-superfamily. Nature. 1994;368(6472):639-43.

81. Culbert AL, Chakkalakal SA, Theosmy EG, Brennan TA, Kaplan FS, Shore EM. Alk2 regulates early chondrogenic fate in fibrodysplasia ossificans progressiva heterotopic endochondral ossification. Stem Cells. 2014;32(5):1289-300.

82. Foley KL, Hebela N, Keenan MA, Pignolo RJ. Histopathology of periarticular non-hereditary heterotopic ossification. Bone. 2018;109:65-70.

83. Fisher TR, Woods CG. Partial rupture of the tendo calcaneus with heterotopic ossification. Report of a case. J Bone Joint Surg Br. 1970;52(2):334-6.

84. Postacchini F, Di Castro A. Subtotal ossification of the Achilles tendon. Case report. Ital J Orthop Traumatol. 1983;9(4):529-32.

85. Sobel E, Giorgini R, Hilfer J, Rostkowski T. Ossification of a ruptured achilles tendon: a case report in a diabetic patient. J Foot Ankle Surg. 2002;41(5):330-4.

86. Peterson JR, De La Rosa S, Sun H, Eboda O, Cilwa KE, Donneys A, et al. Burn injury enhances bone formation in heterotopic ossification model. Ann Surg. 2014;259(5):993-8.

87. van Dinther M, Visser N, de Gorter DJ, Doorn J, Goumans MJ, de Boer J, et al. ALK2 R206H mutation linked to fibrodysplasia ossificans progressiva confers constitutive activity to the BMP type I receptor and sensitizes mesenchymal cells to BMP-induced osteoblast differentiation and bone formation. J Bone Miner Res. 2010;25(6):1208-15.

88. Šošić D, Brand-Saberi B, Schmidt C, Christ B, Olson EN. Regulation of paraxis expression and somite formation by ectoderm- and neural tube-derived signals. Dev Biol. 1997;185(2):229-43.

89. Cserjesi P, Brown D, Ligon KL, Lyons GE, Copeland NG, Gilbert DJ, et al. Scleraxis: a basic helix-loop-helix protein that prefigures skeletal formation during mouse embryogenesis. Development. 1995;121(4):1099-110.

90. Wright E, Hargrave MR, Christiansen J, Cooper L, Kun J, Evans T, et al. The Sry-related gene Sox9 is expressed during chondrogenesis in mouse embryos. Nat Genet. 1995;9(1):15-20.

91. Long F, Zhang XM, Karp S, Yang Y, McMahon AP. Genetic manipulation of hedgehog signaling in the endochondral skeleton reveals a direct role in the regulation of chondrocyte proliferation. Development. 2001;128(24):5099-108.

92. Yang L, Tsang KY, Tang HC, Chan D, Cheah KS. Hypertrophic chondrocytes can become osteoblasts and osteocytes in endochondral bone formation. Proc Natl Acad Sci U S A. 2014;111(33):12097-102.

93. Agarwal S, Loder SJ, Cholok D, Peterson J, Li J, Breuler C, et al. Scleraxis-Lineage Cells Contribute to Ectopic Bone Formation in Muscle and Tendon. Stem Cells. 2017;35(3):705-10.

94. Otsuru S, Overholt KM, Olson TS, Hofmann TJ, Guess AJ, Velazquez VM, et al. Hematopoietic derived cells do not contribute to osteogenesis as osteoblasts. Bone. 2017;94:1-9.

95. Dey D, Bagarova J, Hatsell SJ, Armstrong KA, Huang L, Ermann J, et al. Two tissue-resident progenitor lineages drive distinct phenotypes of heterotopic ossification. Sci Transl Med. 2016;8(366):366ra163.

96. Kan L, Peng CY, McGuire TL, Kessler JA. Glast-expressing progenitor cells contribute to heterotopic ossification. Bone. 2013;53(1):194-203.

97. Kan C, Ding N, Yang J, Tan Z, McGuire TL, Lu H, et al. BMP-dependent, injury-induced stem cell niche as a mechanism of heterotopic ossification. Stem Cell Res Ther. 2019;10(1):14.

98. Olmsted-Davis EA, Salisbury EA, Hoang D, Davis EL, Lazard Z, Sonnet C, et al. Progenitors in Peripheral Nerves Launch Heterotopic Ossification. Stem Cells Transl Med. 2017;6(4):1109-19.

99. Egan KP, Kim JH, Mohler ER, 3rd, Pignolo RJ. Role for circulating osteogenic precursor cells in aortic valvular disease. Arterioscler Thromb Vasc Biol. 2011;31(12):2965-71.

100. Kan L, Liu Y, McGuire TL, Berger DM, Awatramani RB, Dymecki SM, et al. Dysregulation of local stem/progenitor cells as a common cellular mechanism for heterotopic ossification. Stem Cells. 2009;27(1):150-6.

101. Kaplan FS, Glaser DL, Shore EM, Pignolo RJ, Xu M, Zhang Y, et al. Hematopoietic stem-cell contribution to ectopic skeletogenesis. J Bone Joint Surg Am. 2007;89(2):347-57.

102. Suda RK, Billings PC, Egan KP, Kim JH, McCarrick-Walmsley R, Glaser DL, et al. Circulating osteogenic precursor cells in heterotopic bone formation. Stem Cells. 2009;27(9):2209-19.

103. Tseng HW, Girard D, Alexander KA, Millard SM, Torossian F, Anginot A, et al. Spinal cord injury reprograms muscle fibroadipogenic progenitors to form heterotopic bones within muscles. Bone Res. 2022;10(1):22.

104. Chakkalakal SA, Zhang D, Culbert AL, Convente MR, Caron RJ, Wright AC, et al. An Acvr1 R206H knock-in mouse has fibrodysplasia ossificans progressiva. J Bone Miner Res. 2012;27(8):1746-56.

105. Genet F, Kulina I, Vaquette C, Torossian F, Millard S, Pettit AR, et al. Neurological heterotopic ossification following spinal cord injury is triggered by macrophage-mediated inflammation in muscle. The Journal of pathology. 2015;236(2):229-40.

106. Torossian F, Guerton B, Anginot A, Alexander KA, Desterke C, Soave S, et al. Macrophage-derived oncostatin M contributes to human and mouse neurogenic heterotopic ossifications. JCI Insight. 2017;2(21).

107. Gannon FH, Glaser D, Caron R, Thompson LD, Shore EM, Kaplan FS. Mast cell involvement in fibrodysplasia ossificans progressiva. Hum Pathol. 2001;32(8):842-8.

108. Brennan TA, Lindborg CM, Bergbauer CR, Wang H, Kaplan FS, Pignolo RJ. Mast cell inhibition as a therapeutic approach in fibrodysplasia ossificans progressiva (FOP). Bone. 2018;109:259-66.

109. Alexander KA, Tseng HW, Kulina I, Fleming W, Vaquette C, Genêt F, et al. Lymphocytes Are Not Required for Neurogenic Heterotopic Ossification Development after Spinal Cord Injury. Neurotrauma Rep. 2022;3(1):87-96.

110. Ranganathan K, Agarwal S, Cholok D, Loder S, Li J, Sung Hsieh HH, et al. The role of the adaptive immune system in burn-induced heterotopic ossification and mesenchymal cell osteogenic differentiation. J Surg Res. 2016;206(1):53-61.

111. Kan L, Kessler JA. Animal models of typical heterotopic ossification. J Biomed Biotechnol. 2011;2011:309287.

112. Shimono K, Tung WE, Macolino C, Chi AH, Didizian JH, Mundy C, et al. Potent inhibition of heterotopic ossification by nuclear retinoic acid receptor-γ agonists. Nat Med. 2011;17(4):454-60.

113. Chakkalakal SA, Uchibe K, Convente MR, Zhang D, Economides AN, Kaplan FS, et al. Palovarotene Inhibits Heterotopic Ossification and Maintains Limb Mobility and Growth in Mice With the Human ACVR1(R206H) Fibrodysplasia Ossificans Progressiva (FOP) Mutation. J Bone Miner Res. 2016;31(9):1666-75.

114. Hatsell SJ, Idone V, Wolken DM, Huang L, Kim HJ, Wang L, et al. ACVR1R206H receptor mutation causes fibrodysplasia ossificans progressiva by imparting responsiveness to activin A. Sci Transl Med. 2015;7(303):303ra137.

115. Lees-Shepard JB, Yamamoto M, Biswas AA, Stoessel SJ, Nicholas SE, Cogswell CA, et al. Activin-dependent signaling in fibro/adipogenic progenitors causes fibrodysplasia ossificans progressiva. Nat Commun. 2018;9(1):471.

116. Yu PB, Deng DY, Lai CS, Hong CC, Cuny GD, Bouxsein ML, et al. BMP type I receptor inhibition reduces heterotopic [corrected] ossification. Nat Med. 2008;14(12):1363-9.

117. Hamilton PT, Jansen MS, Ganesan S, Benson RE, Hyde-Deruyscher R, Beyer WF, et al. Improved bone morphogenetic protein-2 retention in an injectable collagen matrix using bifunctional peptides. PLoS One. 2013;8(8):e70715.

118. Yano M, Kawao N, Okumoto K, Tamura Y, Okada K, Kaji H. Fibrodysplasia ossificans progressiva-related activated activin-like kinase signaling enhances osteoclast formation during heterotopic ossification in muscle tissues. J Biol Chem. 2014;289(24):16966-77.

119. James AW, Zara JN, Zhang X, Askarinam A, Goyal R, Chiang M, et al. Perivascular stem cells: a prospectively purified mesenchymal stem cell population for bone tissue engineering. Stem Cells Transl Med. 2012;1(6):510-9.

120. Lounev VY, Ramachandran R, Wosczyna MN, Yamamoto M, Maidment AD, Shore EM, et al. Identification of progenitor cells that contribute to heterotopic skeletogenesis. J Bone Joint Surg Am. 2009;91(3):652-63.

121. Rumi MN, Deol GS, Singapuri KP, Pellegrini VD, Jr. The origin of osteoprogenitor cells responsible for heterotopic ossification following hip surgery: an animal model in the rabbit. Journal of orthopaedic research : official publication of the Orthopaedic Research Society. 2005;23(1):34-40.

122. Peterson JR, Okagbare PI, De La Rosa S, Cilwa KE, Perosky JE, Eboda ON, et al. Early detection of burn induced heterotopic ossification using transcutaneous Raman spectroscopy. Bone. 2013;54(1):28-34.

123. Schneider DJ, Moulton MJ, Singapuri K, Chinchilli V, Deol GS, Krenitsky G, et al. The Frank Stinchfield Award. Inhibition of heterotopic ossification with radiation therapy in an animal model. Clin Orthop Relat Res. 1998(355):35-46.

124. Li L, Jiang Y, Lin H, Shen H, Sohn J, Alexander PG, et al. Muscle injury promotes heterotopic ossification by stimulating local bone morphogenetic protein-7 production. J Orthop Translat. 2019;18:142-53.

125. Brady RD, Zhao MZ, Wong KR, Casilla-Espinosa PM, Yamakawa GR, Wortman RC, et al. A novel rat model of heterotopic ossification after polytrauma with traumatic brain injury. Bone. 2020;133:115263.

126. Kang H, Dang AB, Joshi SK, Halloran B, Nissenson R, Zhang X, et al. Novel mouse model of spinal cord injury-induced heterotopic ossification. J Rehabil Res Dev. 2014;51(7):1109-18.

127. Wang Y, Lu J, Liu Y. Skeletal Muscle Regeneration in Cardiotoxin-Induced Muscle Injury Models. Int J Mol Sci. 2022;23(21).

128. Freehafer AA, Yurick R, Mast WA. Para-articular ossification in spinal cord injury. Med Serv J Can. 1966;22(7):471-8.

129. Miller LF, O'Neill CJ. Myositis ossificans in paraplegics. JBJS. 1949;31(2):283-94.

130. Rossier A, Bussat P, Infante F, Zender R, Courvoisier B, Muheim G, et al. Current facts on para-osteo-arthropathy (POA). Spinal Cord. 1973;11(1):36-78.

131. Genêt F, Jourdan C, Schnitzler A, Lautridou C, Guillemot D, Judet T, et al. Troublesome heterotopic ossification after central nervous system damage: a survey of 570 surgeries. PLoS One. 2011;6(1):e16632.

132. Sullivan MP, Torres SJ, Mehta S, Ahn J. Heterotopic ossification after central nervous system trauma: A current review. Bone Joint Res. 2013;2(3):51-7.

133. Aubut JA, Mehta S, Cullen N, Teasell RW. A comparison of heterotopic ossification treatment within the traumatic brain and spinal cord injured population: An evidence based systematic review. NeuroRehabilitation. 2011;28(2):151-60.

134. Banovac K, Gonzalez F. Evaluation and management of heterotopic ossification in patients with spinal cord injury. Spinal Cord. 1997;35(3):158-62.

135. van Kuijk AA, Geurts AC, van Kuppevelt HJ. Neurogenic heterotopic ossification in spinal cord injury. Spinal Cord. 2002;40(7):313-26.

136. Meyers C, Lisiecki J, Miller S, Levin A, Fayad L, Ding C, et al. Heterotopic Ossification: A Comprehensive Review. JBMR Plus. 2019;3(4):e10172-e.

137. Banovac K, Sherman AL, Estores IM, Banovac F. Prevention and treatment of heterotopic ossification after spinal cord injury. J Spinal Cord Med. 2004;27(4):376-82.

138. Ampadiotaki MM, Evangelopoulos DS, Pallis D, Vlachos C, Vlamis J, Evangelopoulos ME. New Strategies in Neurogenic Heterotopic Ossification. Cureus. 2021;13(4):e14709.

139. Genêt F, Denormandie P, Keenan MA. Orthopaedic surgery for patients with central nervous system lesions: Concepts and techniques. Ann Phys Rehabil Med. 2019;62(4):225-33.

140. Gao C, Chen BP, Sullivan MB, Hui J, Ouellet JA, Henderson JE, et al. Micro CT Analysis of Spine Architecture in a Mouse Model of Scoliosis. Front Endocrinol (Lausanne). 2015;6:38.

141. Campbell GM, Sophocleous A. Quantitative analysis of bone and soft tissue by micro-computed tomography: applications to ex vivo and in vivo studies. Bonekey Rep. 2014;3:564.

142. Eckardt JJ, Ivins JC, Perry HO, Unni KK. Osteosarcoma arising in heterotopic ossification of dermatomyositis: Case report and review of the literature. Cancer. 1981;48(5):1256-61.

143. Fournier DE, Kiser PK, Beach RJ, Dixon SJ, Séguin CA. Dystrophic calcification and heterotopic ossification in fibrocartilaginous tissues of the spine in diffuse idiopathic skeletal hyperostosis (DISH). Bone Research. 2020;8(1):16.

144. Li L, Xiang S, Wang B, Lin H, Cao G, Alexander PG, et al. Dead muscle tissue promotes dystrophic calcification by lowering circulating TGF-β1 level. Bone Joint Res. 2020;9(11):742-50.

145. Rajagopalan S. Crush Injuries and the Crush Syndrome. Med J Armed Forces India. 2010;66(4):317-20.

146. Li L, Xiang S, Wang B, Lin H, Kihara S, Sun H, et al. TGF-β1 plays a protective role in glucocorticoid-induced dystrophic calcification. Bone. 2020;136:115355.

147. Tőkési N, Kozák E, Fülöp K, Dedinszki D, Hegedűs N, Király B, et al. Pyrophosphate therapy prevents trauma-induced calcification in the mouse model of neurogenic heterotopic ossification. J Cell Mol Med. 2020.

148. Mignemi NA, Yuasa M, Baker CE, Moore SN, Ihejirika RC, Oelsner WK, et al. Plasmin Prevents Dystrophic Calcification After Muscle Injury. Journal of bone and mineral research : the official journal of the American Society for Bone and Mineral Research. 2017;32(2):294-308.

149. Ripamonti U. Osteoinduction in porous hydroxyapatite implanted in heterotopic sites of different animal models. Biomaterials. 1996;17(1):31-5.

150. Hayman AR. Tartrate-resistant acid phosphatase (TRAP) and the osteoclast/immune cell dichotomy. Autoimmunity. 2008;41(3):218-23.

151. Moore-Lotridge SN, Li Q, Gibson BHY, Martin JT, Hawley GD, Arnold TH, et al. Trauma-Induced Nanohydroxyapatite Deposition in Skeletal Muscle is Sufficient to Drive Heterotopic Ossification. Calcified tissue international. 2019;104(4):411-25.

152. Yao Y, Cai X, Ren F, Ye Y, Wang F, Zheng C, et al. The Macrophage-Osteoclast Axis in Osteoimmunity and Osteo-Related Diseases. Front Immunol. 2021;12:664871.

153. Alexander KA, Tseng HW, Fleming W, Jose B, Salga M, Kulina I, et al. Inhibition of JAK1/2 Tyrosine Kinases Reduces Neurogenic Heterotopic Ossification After Spinal Cord Injury. Frontiers in immunology. 2019;10:377.

154. Lampiasi N, Russo R, Zito F. The Alternative Faces of Macrophage Generate Osteoclasts. BioMed research international. 2016;2016:9089610.

155. Yahara Y, Nguyen T, Ishikawa K, Kamei K, Alman BA. The origins and roles of osteoclasts in bone development, homeostasis and repair. Development. 2022;149(8).

156. Battaglino RA, Lazzari AA, Garshick E, Morse LR. Spinal cord injury-induced osteoporosis: pathogenesis and emerging therapies. Curr Osteoporos Rep. 2012;10(4):278-85.

157. Hook MA, Falck A, Dundumulla R, Terminel M, Cunningham R, Sefiani A, et al. Osteopenia in a Mouse Model of Spinal Cord Injury: Effects of Age, Sex and Motor Function. Biology (Basel). 2022;11(2).

158. Shams R, Drasites KP, Zaman V, Matzelle D, Shields DC, Garner DP, et al. The Pathophysiology of Osteoporosis after Spinal Cord Injury. Int J Mol Sci. 2021;22(6).

159. Kurer MH, Khoker MA, Dandona P. Human osteoblast stimulation by sera from paraplegic patients with heterotopic ossification. Paraplegia. 1992;30(3):165-8.

160. Bidner SM, Rubins IM, Desjardins JV, Zukor DJ, Goltzman D. Evidence for a humoral mechanism for enhanced osteogenesis after head injury. J Bone Joint Surg Am. 1990;72(8):1144-9.

161. Cadosch D, Toffoli AM, Gautschi OP, Frey SP, Zellweger R, Skirving AP, et al. Serum after traumatic brain injury increases proliferation and supports expression of osteoblast markers in muscle cells. J Bone Joint Surg Am. 2010;92(3):645-53.

162. Lee S, Hwang C, Marini S, Tower RJ, Qin Q, Negri S, et al. NGF-TrkA signaling dictates neural ingrowth and aberrant osteochondral differentiation after soft tissue trauma. Nat Commun. 2021;12(1):4939.

163. Tuzmen C, Verdelis K, Weiss L, Campbell P. Crosstalk between substance P and calcitonin gene-related peptide during heterotopic ossification in murine Achilles tendon. Journal of orthopaedic research : official publication of the Orthopaedic Research Society. 2018;36(5):1444-55.

164. Zhang Q, Zhou D, Wang H, Tan J. Heterotopic ossification of tendon and ligament. J Cell Mol Med. 2020;24(10):5428-37.

165. Salisbury E, Rodenberg E, Sonnet C, Hipp J, Gannon FH, Vadakkan TJ, et al. Sensory nerve induced inflammation contributes to heterotopic ossification. Journal of cellular biochemistry. 2011;112(10):2748-58.

166. Sang X, Wang Z, Shi P, Li Y, Cheng L. CGRP accelerates the pathogenesis of neurological heterotopic ossification following spinal cord injury. Artif Cells Nanomed Biotechnol. 2019;47(1):2569-74.

167. Lim DJ. Intraoperative finding and management of complete spinal cord transection after thoracolumbar traumatic fracture-dislocation: A case report. Medicine (Baltimore). 2021;100(2):e24096.

168. Raguindin PF, Muka T, Glisic M. Sex and gender gap in spinal cord injury research: Focus on cardiometabolic diseases. A mini review. Maturitas. 2021;147:14-8.

169. Weld KJ, Dmochowski RR. Effect of bladder management on urological complications in spinal cord injured patients. J Urol. 2000;163(3):768-72.

170. Wada N, Shimizu T, Takai S, Shimizu N, Kanai AJ, Tyagi P, et al. Post-injury bladder management strategy influences lower urinary tract dysfunction in the mouse model of spinal cord injury. Neurourol Urodyn. 2017;36(5):1301-5.

171. Foster AD. The impact of bipedal mechanical loading history on longitudinal long bone growth. PLoS One. 2019;14(2):e0211692.

172. Ferguson VL, Ayers RA, Bateman TA, Simske SJ. Bone development and age-related bone loss in male C57BL/6J mice. Bone. 2003;33(3):387-98.

A thesis submitted to McGill University in partial fulfillment of the requirements for the degree of Master of Science in Experimental Surgery